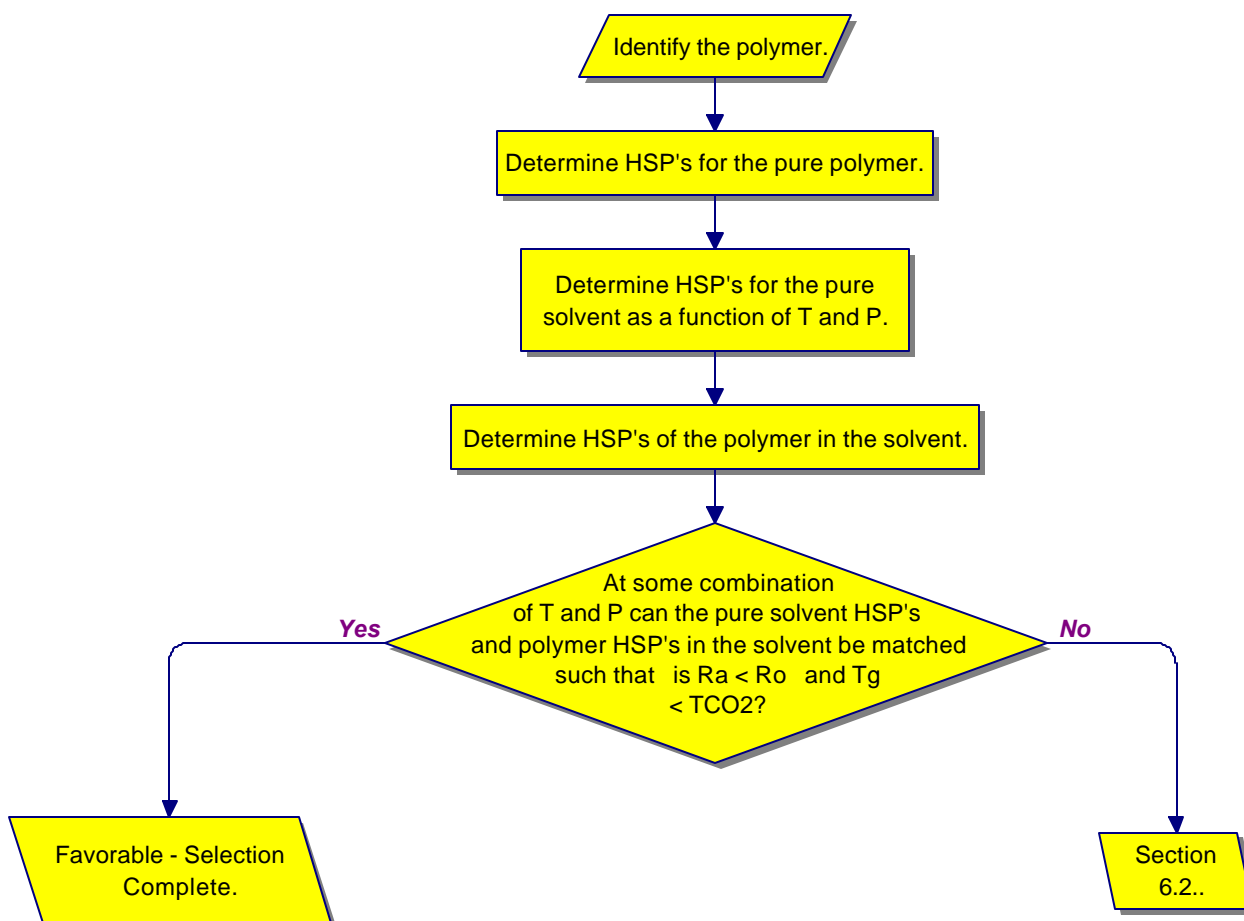# 6   Binary Interactions

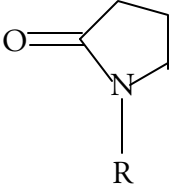## 6.1   Solvent/Polymer Interactions

Figure 6-1. *Decision tree for the section of an optimum solvent for a desired polymer interaction.*

The removal of polymer coatings with a (supercritical) solvent is dependent on sorption of the solvent into the polymer, and therefore on favorable intermolecular interactions. Predicting and optimizing this sorption means producing conditions giving the best match between the solubility parameters of the solvent (CO_2) and the polymer. This will require knowledge of the chemical and physical characteristics of the polymer.
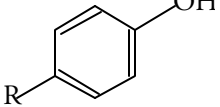
The ability of a polymer to solublize CO_2 depends on its chemical structure. For example, it has been shown that polymers possessing electron-donating (Lewis base) functional groups exhibit specific (attractive) interactions with CO_2.[374] In theory, the presence and strength of an acid-base interaction can be predicted from the type, number, and location of functional groups within a given polymer. Many industrial polymers contain pyrrolidone, ether, nitrile, carbonyl, siloxane, or fluorine groups that act as proton acceptors (Lewis bases) in the presence of CO_2, or hydroxyl, phenol, sulfonic acid, or carboxyl groups that act as proton donors (Lewis acids) in a CO_2 environment.[375] Table 6-1 illustrates these functional groups.

**Table 6-1.** *Common polymer functional groups and their Lewis acid-base behavior in the presence of CO_2.*

Lewis Base Functional Groups

Pyrrolidone	Ether	Nitrile	Carbonyl	Siloxane	Fluorine
	C—O—C with R groups	N≡C—C—R	R—C(=O)—R	Si—O with R groups	R—F

Lewis Acid Functional Groups

Hydroxyl	Phenol	Sulfonic Acid	Carboxyl
R—OH		R—S(=O)(=O)—OH	R—C(=O)—OH
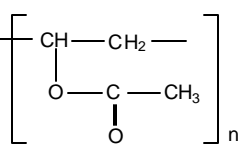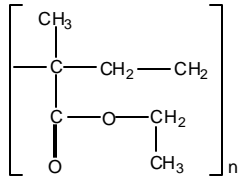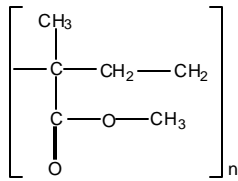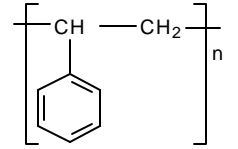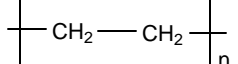
As an example of specific intermolecular interactions, it has been documented that the presence of a carbonyl group in a polymer enhances the solubility of CO_2.[376,377,378,379,380,381,382,383,384] There is spectroscopic evidence that the interaction of the carbonyl oxygen (acting as a Lewis base) with the carbon atom of CO_2 (acting as a Lewis acid), produces an ordered "complex" in one of the two configurations shown in Figure 6-2.

(a)   (b)
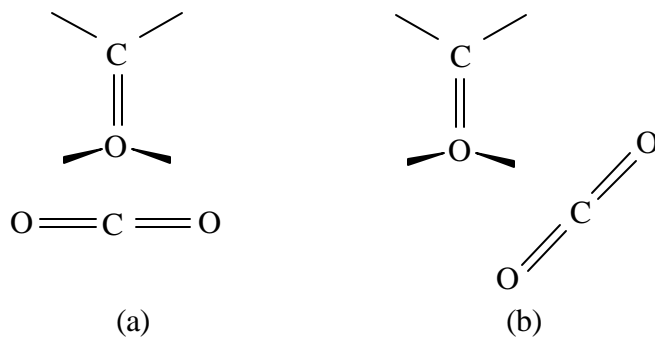
Figure 6-2. *Proposed physical configuration produced by Lewis acid-base interaction between CO_2 and polymeric carbonyl functional group.*[385]

The evidence for this type of interaction was found by Kazarian and coworkers[386] using Fourier transform infrared spectroscopy. Details of this work can be found in the indicated reference, but the general results support the importance of Lewis base functional groups, and particularly the carbonyl functional group, in the strength of a Lewis acid-base type interaction with CO_2, and the resulting enhancement of CO_2 solubility. Table 6-2 lists the polymers evaluated by Kazarian in the order of decreasing CO_2 interaction strength (based on the change in the CO_2 bending mode frequency). Also included in the table, for comparison, is CO_2 sorption data at comparable temperature and pressure conditions. It is noted in the table whether the sorption data was measured in-situ (at pressure and temperature), or ex-situ (immediately following depressurization). It was noted by Kazarian in this work that the higher sorption of CO_2 with poly(styrene) compared to poly(ethylene) is due a weak acid/base interaction electrostatic interactions of CO_2 with the benzyl group in polystyrene, acting as a weak Lewis base.

Table 6-2. *Strength of interaction of CO_2 with polymers containing Lewis base groups, as measured by molecular bending mode frequency, $\Delta\nu_{1/2}$, and measured CO_2 solubility, $[CO_2]$.*

Polymer	Monomer Structure	$\Delta\nu_{1/2}$ (cm^{-1})[387]	$[CO_2] \cdot 10^3$ $(\text{moles } CO_2/cm^3 \text{ polymer})$
Poly(vinyl acetate)- PVA	CH—CH₂— / O—C—CH₃ / O	16	$13.1^{[388]}$ (in-situ) ($25^{o}C$, 65.5 bar) $6.16^{[389]}$ (in-situ) ($47^{o}C$, 60 bar)
Poly(ethyl methylacrylate) – PEMA	CH₃ / C—CH₂—CH₂ / C—O—CH₂ / O CH₃	15	$4.09^{[390]}$ (in-situ) ($35^{o}C$, 44.5 bar) $2.50^{[391]}$ (in-situ) ($55^{o}C$, 44.5 bar)
Poly(methyl methylacrylate) – PMMA	CH₃ / C—CH₂—CH₂ / C—O—CH₃ / O	15	$3.86^{[392]}$ (in-situ) ($35^{o}C$, 50 bar) $2.18^{[393]}$ (in-situ) ($65^{o}C$, 50 bar)
Poly(styrene) – PS	CH—CH₂ (phenyl ring)	0	$2.03^{[394]}$ (in-situ) ($35^{o}C$, 51 bar) $1.48^{[395]}$ (in-situ) ($50^{o}C$, 51 bar)
Poly(ethylene) – PE	CH₂—CH₂	0	$0.12^{[396]}$ (ex-situ) ($40^{o}C$, 69 bar)

The location of the functional group within a polymer also affects the amount of CO_2 sorption,[397] as seen in the example of CO_2 uptake in poly(methyl methacrylate) (PMMA) and glycol modified poly(ethylene terephthalate) (PETG), Figure 6-3.   In this study, PMMA showed greater CO_2 solubility than PETG, despite the higher T_g for PMMA ($105^{o}C$ vs $79^{o}C$). Because both materials were amorphous, it was hypothesized that the presence of the side-chain ester functionality, as compared to the main-chain ester functionality of PETG allows for greater dissolution of CO_2 in PMMA. [398]   In the

work of Kirby and McHugh,[399] the effects of chain branching were observed to increase solubility in two ways; through an increase in the free volume of the polymer, which makes it easier to absorb solvent, and in a reduction of intermolecular interactions between polymer segments which arise in linear segments due to short-range molecular orientation.

In the case of structurally similar polymers such as PVA and PMMA, Table 6-2, the polymer having the lower glass transition temperature shows greater CO_2 solubility. PVA, with $T_g = 30^oC$, has a significantly higher solubility for CO_2 than PMMA, with

PMMA   **PETG**
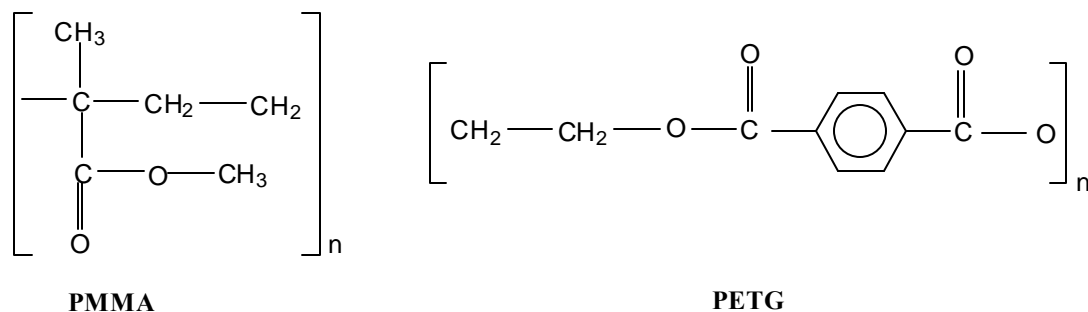
Figure 6-3. Monomer structures of Poly(methyl methacrylate) (PMMA), $T_g = 105^oC$, and Glycol Modified Poly(ethylene terephthalate) (PETG), $T_g = 79^oC$.

$T_g = 105^oC$. Unlike the PMMA and PETG case where the increased solubility can be related to increase free volume, the increased solubility between two (in this case branched) polymers with similar structures can be correlated with a lower cohesive energy density, for which T_g can be used as a indicator, as discussed in Section 5.5.2

There have been many studies on the sorption of CO_2 in polymers, although the temperatures and pressures where these experiments have been conducted are generally below the critical point of CO_2 (31^oC, 73.8 bar). Table 6-3 is a compilation of reported CO_2 solubilities in various polymers. Only the maximum CO_2 concentration at the

experimental conditions of temperature and pressure has been listed, although additional solubility data at other conditions of T and P can be found in the noted references. In addition, the monomer structure of each polymer is shown, as well as the ambient condition values of the polymer T_g) and HSP's. The Hansen solubility parameter values given for CO_2 were determined as in Section 5.3, at the temperature and pressure conditions for which the absorbed CO_2 concentration is given.
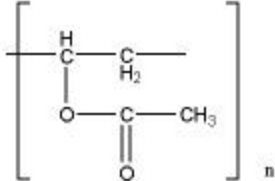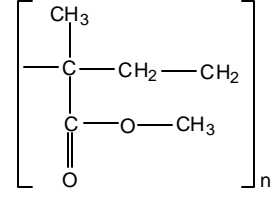
Because the data shown in Table 6-3 were measured using different experimental techniques, and at different conditions of temperature and pressure, direct comparisons are difficult. Furthermore, the polymer processing history, as well as size and geometry of the samples are not included in the comparison. Nevertheless, some general observations from the data in Table 6-3 can be made:
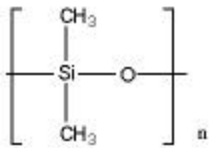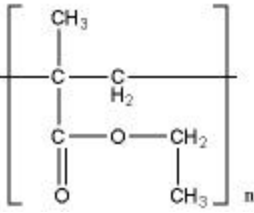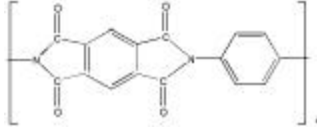
1. In the case of structurally similar polymers, polymers with lower T_g's favor CO_2 solubility. Poly(vinyl acetate), with a low T_g, solubilizes nearly three times more CO_2 than poly(methyl methacrylate) or poly(ethyl methacrylate) at the same temperature and pressure. Stated another way, all other things being equal, a low T_g indicates low intra-molecular interactions, and therefore lower cohesive energy densities.

2. Silicone containing (Lewis base) polymers, which exhibit weak polymer-polymer interactions, as evidenced by the low HSP values and T_g of poly(dimethyl siloxane), favor CO_2 sorption, indicating that the presence of Lewis base groups, in the absence of interfering intra-molecular interactions within the polymer promote CO_2 sorption.
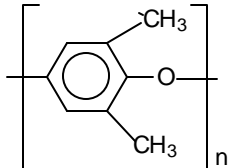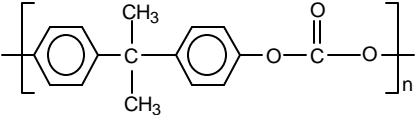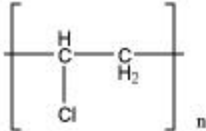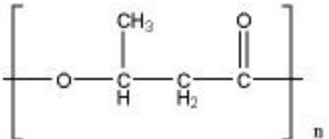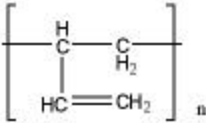
3. Hydrocarbon polymers, such as polybutadiene and polypropylene, show lower uptake of CO_2 per unit of polymer, despite relatively low polymer-polymer interaction (as evidenced by the low HSP values and low T_g for both polymers. This indicates that the absence of Lewis base groups, even without interfering intra-molecular interactions within the polymer, results in low CO_2 solubilities.

4. When Lewis base functional groups are present, their location on a side-chain versus the main-chain favors higher CO_2 solubilities.

Table 6-3. *Maximum solubilities of CO_2 in various polymers.*

Polymer	Monomer Structure	T_g (°C) (25°C, 1 atm)	Polymer (d_d, d_p, d_h) $(MPa)^{1/2}$ (25°C, 1 atm)	T (°C)	P (bar)	$[CO_2] \cdot 10^{-3}$ (moles CO_2/cm³ polymer)	CO_2 (d_d, d_p, d_h) $(MPa)^{1/2}$
Poly(vinyl acetate) – PVA	(structure)	30	$d_d = 16.0$ $d_p = 6.8$ $d_h = 9.8$[400]	25	51	9.03[401]	$d_d = 1.4$ $d_p = 2.0$ $d_h = 2.2$
Poly(methyl methacrylate) - PMMA	(structure)	105	$d_d = 17.6$ $d_p = 7.1$ $d_h = 5.0$[402]	32.7	102.5	6.5[403]	$d_d = 9.5,$ $d_p = 4.2$ $d_h = 4.7$
				35	216.2	13.6[404]	$d_d = 11.5$ $d_p = 4.6$ $d_h = 5.1$
				50	286.5	12.3[405]	$d_d = 11.3$ $d_p = 4.6$ $d_h = 4.9$
				35	50	3.86[406]	$d_d = 1.0$ $d_p = 1.7$ $d_h = 1.9$

Polymer	Monomer Structure	T_g (°C) (25°C, 1 atm)	Polymer (d_l, d_p, d_h) $(MPa)^{1/2}$ (25°C, 1 atm)	T (°C)	P (bar)	$[CO_2] \cdot 10^{-3}$ (moles CO_2/cm^3 polymer)	CO_2 (d_l, d_p, d_h) $(MPa)^{1/2}$
Poly(dimethyl siloxane) - PDMS		-128	$d_l = 15.5$ $d_p = 0$ $d_h = 0$[407]	50	120	8.53[408]	$d_l = 7.1$ $d_p = 3.8$ $d_h = 4.1$
				25	50.7	5.45[409]	$d_l = 1.4$ $d_p = 2.0$ $d_h = 2.2$
				42	220	34.54[410]	$d_l = 10.9$ $d_p = 4.5$ $d_h = 4.9$
Poly(ethyl methacrylate) – PEMA		66	$d_l = 17.8$ $d_p = 6.5$ $d_h = 4.7$[411]	35	50	3.85[412]	$d_l = 1.0$ $d_p = 1.7$ $d_h = 1.9$
				55	44.5	2.50[413]	$d_l = 0.7$ $d_p = 1.5$ $d_h = 1.6$
Polyimide - PI		227	$d_l = 19.6$ $d_p = 7.6$ $d_h = 9.0$[414]	40	96.5	3.63[415]	$d_l = 7.1$ $d_p = 3.8$ $d_h = 4.1$

Polymer	Monomer Structure	T_g (°C) (25°C, 1 atm)	Polymer (d_l, d_p, d_h) $(MPa)^{1/2}$ (25°C, 1 atm)	T (°C)	P (bar)	$[CO_2] \cdot 10^{-3}$ (moles CO_2/cm³ polymer)	CO_2 (d_l, d_p, d_h) $(MPa)^{1/2}$
Poly(2, 6-dimethyl phenylene oxide) - PPO		216	$d_l = 18.0$ $d_p = 3.1$ $d_h = 8.5$[416]	35	40.5	2.36[417]	$d_d = 0.8$ $d_p = 1.6$ $d_h = 1.7$
Polycarbonate - PC		150	$d_l = 18.1$ $d_p = 5.9$ $d_h = 6.9$[418]	40	96.5	3.27[419]	$d_d = 7.1$ $d_p = 3.8$ $d_h = 4.1$
				35	271	4.1[420]	$d_d = 12.1$ $d_p = 4.7$ $d_h = 5.2$
Poly(vinyl chloride) - PVC		85	$d_l = 18.8$ $d_p = 10.0$ $d_h = 3.1$[421]	35	20.3	0.86[422] (ex-situ)	$d_d = 0.2$ $d_p = 1.0$ $d_h = 1.1$
				25	63.8	2.49[423]	$d_d = 2.8$ $d_p = 2.6$ $d_h = 2.9$
Poly(hydroxy butyrate) - PHB			$d_l = 16.0$ $d_p = 11.9$ $d_h = 8.3$[424]	35	60	2.38[425]	$d_d = 1.4$ $d_p = 2.0$ $d_h = 2.2$
Polybutadiene - PB		-25	$d_l = 17.5$ $d_p = 0$ $d_h = 1.0$[426]	25	50.7	2.54[427]	$d_d = 1.4$ $d_p = 2.0$ $d_h = 2.2$

Polymer	Monomer Structure	Tg (°C) (25°C, 1 atm)	Polymer (d_l, d_p, d_h) (MPa)$^{1/2}$ (25°C, 1 atm)	T (°C)	P (bar)	$[CO_2] \cdot 10^{-3}$ (moles CO_2/cm^3 polymer)	CO_2 (d_l, d_p, d_h) (MPa)$^{1/2}$
Poly(ethylene terephthalate) - PET		74	$d_l = 19.4$ $d_p = 6.2$ $d_h = 8.6$[428]	35	60.8	2.19[429]	$d_l = 1.4$ $d_p = 2.0$ $d_h = 2.2$
Polystyrene - PS		100	$d_l = 21.3$ $d_p = 5.8$ $d_h = 4.3$[430]	35	71	2.77[431]	$d_l = 2.3$ $d_p = 2.5$ $d_h = 2.7$
				40	165	3.34[432]	$d_l = 10.3$ $d_p = 4.4$ $d_h = 4.8$
Poly(vinyl butyral) – PVB		55-90	$d_l = 17.4$ $d_p = 8.8$ $d_h = 11.3$[433]	25	35.5	2.04[434]	$d_l = 0.6$ $d_p = 1.4$ $d_h = 1.5$
Poly(vinyl alcohol) - PVOH		85	$d_l = 17.8$ $d_p = 9.0$ $d_h = 18.0$[435]	47	60	1.61[436]	$d_l = 1.2$ $d_p = 1.9$ $d_h = 2.0$
				35	60	1.01[437]	$d_l = 1.4$ $d_p = 2.0$ $d_h = 2.2$
Polypropylene - PP		-14	$d_l = 17.2$ $d_p = 0$ $d_h = 0$[438]	25	50.7	0.73[439] (in-situ)	$d_l = 1.4$ $d_p = 2.0$ $d_h = 2.2$

With the exception of the noted value for PVC, all CO_2 sorption values are in-situ.

Factors not considered in the analysis of the CO_2 sorption values in Table 6-3 include the temperature and hydrostatic pressure effects on the polymer HSP values, polymer swelling resulting from CO_2 sorption, and the difference between the density of the CO_2 absorbed within the polymer (i.e., partial molar volume) and the density of the CO_2 in the gas phase.

As discussed in Section 5.5.3, polymer HSP's can be adjusted for temperature and hydrostatic pressure using experimental PVT data, empirical equations of state, or representative coefficients of thermal expansion and compressibility. In addition to these two effects, which occur for all polymers and in all environments, polymer swelling due to CO_2 sorption will result in increased distances between polymer segments, and therefore an increased polymer specific volume. This will lower the cohesive energy density and HSP's of the polymer. To evaluate the magnitude of the increase and/or decrease in polymer HSP's with T, P, and CO_2 sorption, it is proposed that the effects on polymer specific volume are separable and additive, i.e.,

$$V^{T,P} = V_o^{T_0,P_0} + \Delta V^{T-T_0} + \Delta V^{P-P_0} + \Delta V^{CO_2\,sorption} \tag{6-1}$$

where $V_o^{T_0,P_0}$ is the polymer specific volume at ambient conditions (normally 25°C and 1 atmosphere), ΔV^{T-T_0} is the change in the polymer specific volume due to a change in temperature, ΔV^{P-P_0} is the change in the polymer specific volume due to a change in hydrostatic pressure, and $\Delta V^{CO_2\,sorption}$ is the increase in polymer specific volume due to the sorption of CO_2 at T and P.

The sorption of CO_2 results in a change in polymer volume only when the polymer is in its rubber state, i.e., when the sorption temperature is above T_g. However, as discussed in Section 2.2.5, the sorption of CO_2 will lower the polymer T_g. It is therefore necessary to be able to predict whether a polymer will be in the glass or rubber state at the sorption conditions. The observed change in T_g with CO_2 sorption, $\left(\dfrac{dT_g}{dP} \right)_{Observed}$, incorporates the effect of two separate contributions: an increase in T_g caused by hydrostatic compression, $\left(\dfrac{dT_g}{dP} \right)_{Hydrostatic}$, and a decrease in T_g caused by swelling due to gas sorption, $\left(\dfrac{dT_g}{dP} \right)_{Swelling}$, i.e.

$$\left(\frac{dT_g}{dP} \right)_{Observed} = \left(\frac{dT_g}{dP} \right)_{Hydrostatic} + \left(\frac{dT_g}{dP} \right)_{Swelling} \tag{6-2}$$
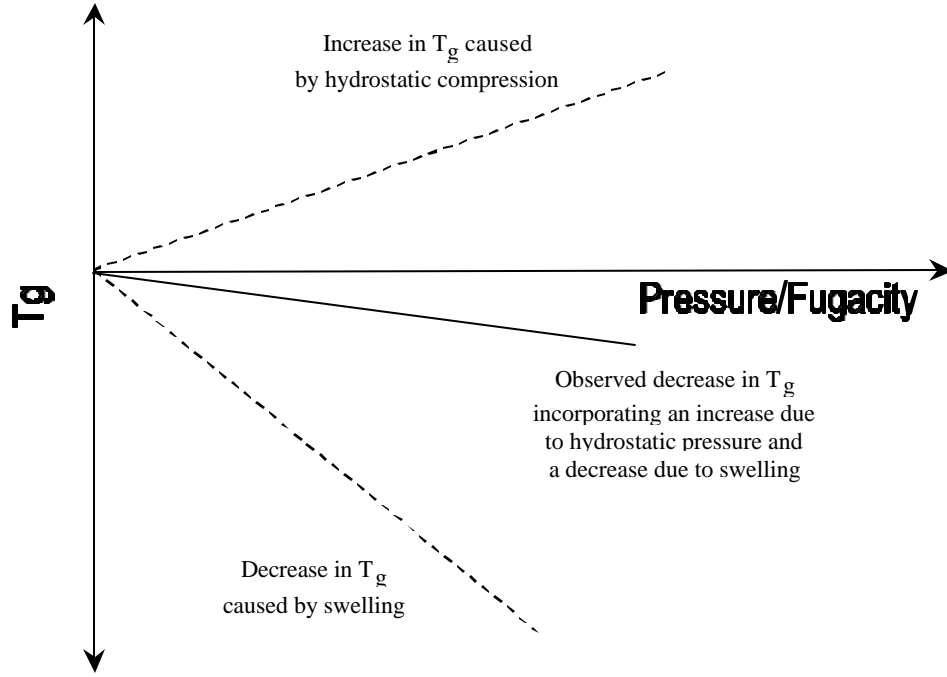
Figure 6-4. *Schematic illustration of the observed change in polymer T_g when exposed to pressurized, penetrating gas (at constant temperature). This observed change incorporates two separate effects: An increase in T_g due to hydrostatic compression and a decrease due to swelling. For a non-penetrating fluid, only the increase in T_g will be observed.*

The volume fraction of absorbed CO_2, $[CO_2]$, can be approximated using the dual mode sorption model,[440,441,442,443]

$$C\left(\frac{cm^3 \ CO_2}{cm^3 \ polymer}\right) = C_D + C_H = k_D P + \frac{C_H^{'} bP}{1 + bP} \tag{6-3}$$

where $k_D P$ is the linear sorption term (Henry's law relationship) and $\dfrac{C_H^{'} bP}{1 + bP}$ the Langmuir sorption term. The Langmuir sorption term corresponds to hole filling in the glass state and does not contribute to overall volume dilation of the polymer. The presence of the Langmuir sorption sites in a polymer is connected with the existence of a nonequilibrium free volume at temperatures below the glass transition temperature in the

polymer matrix.[444]   For $T > T_g$, the volume fraction of absorbed CO_2 can therefore be expressed by the linear sorption term, $k_D P$.

$$C\left(\frac{cm^3 \ CO_2}{cm^3 \ polymer}\right) = C_D = k_D P \tag{6-4}$$

This is a Henry's law-type relationship, where k_D is analogous to the Henry's law constant.[445]. This relation is discussed further in Appendix B.

In theory, therefore, the increase in polymer volume due to absorbed CO_2, $\Delta V^{CO_2 \ sorption}$, can be found by multiplying the volume fraction of absorbed CO_2, $[CO_2]$ by its partial molar volume at the sorption conditions, $\overline{V}_{CO_2}$, the volume of a mole of ideal gas at 0°C and 1 atm and the specific volume of the unswollen polymer, $V^o_{polymer}$ [446]

$$\Delta V^{CO_2} = [CO_2] \cdot \frac{\overline{V}_{CO_2}}{22415} V^o_{polymer} \tag{6-5}$$

where 22,415 is the volume of 1 mole of ideal gas at 0°C and 1 atm.[447]

Combining eqns. (6-2) and (6-5),

$$\Delta V^{CO_2} = k_D P \cdot \left(\frac{\overline{V}_{CO_2}}{22415}\right) \cdot V^0_{Polymer} \tag{6-6}$$

so that

$$\boxed{\frac{\Delta V^{CO_2}}{V^0_{Polymer}} = k_D P \cdot \left(\frac{\overline{V}_{CO_2}}{22415}\right)} \tag{6-7}$$

Equation (6-7) was derived by Fleming and Koros[448] to determine the volume increase of polymers due to sorption of CO_2, where V_o is the unswollen polymer volume, and the partial molar volume of CO_2 was taken by these authors to be $\overline{V}_{CO_2} = 46 \left(cm^3\!\big/_{mole} \right)$. This value of $\overline{V}_{CO_2}$ was obtained by averaging the values of CO_2 partial molar volume in six liquid solvents (at 25^oC). The list of solvents used by Fleming and Koros to determine their $\overline{V}_{CO_2}$ is reproduced in Table 6-4.

Table 6-4. *Partial molar volume of CO_2 in various liquids at 25^oC.*

Solvent	$\overline{V}_{CO_2} \left(cm^3\!\big/_{mole} \right)$
Carbon tetrachloride	48.2
Chlorobenzene	44.6
Benzene	47.9
Acetone	44.7
Methyl acetate	44.5
Methanol	43.0
	Avg. $\overline{V}_{CO_2} = 46.0$

An expanded tabulation of CO_2 partial molar volumes in various liquid solvents, as reported in the literature at $p_{CO_2} = 1$ atm and 25^oC, is given in Table 6-5.

Table 6-5 *Partial Molar Volume of CO_2 in Various Liquids, $p_{CO_2} = 1$ atm, $T = 25^oC$.*

$\overline{V}_{CO_2}$ (cm^3/mole)	Solvent	V_{m1} (cm^3/mole) solvent	δ_d (MPa)$^{1/2}$	δ_p (MPa)$^{1/2}$	δ_h (MPa)$^{1/2}$	δ_T (MPa)$^{1/2}$	Ref
33	water	17.54	15.5	16.0	42.3	47.8	449
33.5	n-formyl morpholine	100.82	16.6	11.7	10.0	22.6	450
35	water	17.54	15.5	16.0	42.3	47.8	451
35.6	n-formyl morpholine	100.82	16.6	11.7	10.0	22.6	452
42.2	propylene carbonate	85.08	20.0	18.0	4.1	27.2	453
43	methanol	40.71	15.1	12.3	22.3	29.6	454
44.2	methyl acetate	79.91	15.5	7.2	7.6	18.7	455
44.4	chlorobenzene	102.23	19.0	4.3	2.0	19.6	456
44.4	acetone	73.89	15.5	10.4	7.0	19.9	457
44.7	acetone	73.89	15.5	10.4	7.0	19.9	458

45.9	methylbenzene	106.52	18.0	1.4	2.0	18.2	459
47.6	benzene	89.48	18.4	0.0	2.0	18.5	460
47.9	tetrachloromethane	97.17	17.8	0.0	0.6	17.8	461
48.0	hexadecane	294.08	16.3	0.0	0.0	16.3	462
48.4	tetradecane	261.73	16.2	0.0	0.0	16.2	463
48.9	dodecane	229.64	16.0	0.0	0.0	16.0	464
49.7	decane	195.44	15.7	0.0	0.0	15.7	465
50.8	nonane	179.38	15.7	0.0	0.0	15.7	466
51.3	cyclohexane	108.88	16.8	0.0	0.0	16.8	467
52.0	methylcyclohexane	128.18	16.0	0.0	1.0	16.0	468
52.1	octane	163.42	15.5	0.0	0.0	15.5	469
52.7	heptane	146.93	15.3	0.0	0.0	15.3	470
69	perfluoroheptane	227.3	12.0	0.0	0.0	12	471

A more accurate value for the partial molar volume of CO_2 dissolved in a polymer, over that used by Fleming and Koros, can be obtained by using an EOS of CO_2, eqn. (5-14) and eqn. (5-12), and the internal pressure of the polymer, as discussed in Section 4.1. It is proposed that the condition of equilibrium of an inert gas dissolved in a non-polar polymer can be expressed as

$$T\left(\frac{\partial P}{\partial T}\right)_V^{Solute} - P = T\left(\frac{\partial P}{\partial T}\right)_V^{Solvent} - P \qquad (6\text{-}8)$$

This is a similar approach to that used in Section 5.2.1, where the HSP's of CO_2 were determined by an optimization based on solubility in liquid solvents. The implicit assumption in that approach is that the cohesive energy density of the CO_2 and the liquid solvent in which CO_2 was most soluble are equal.

The internal pressure of the polymer of interest, $T\left(\frac{\partial P}{\partial T}\right)_V - P$, can be calculated using the techniques outline in Section 5.5.1: Using measured PVT data, empirical PVT

equations of state, total solubility parameter, $(n \cdot d_{Total}^2)$, or the appropriate values of thermal expansion coefficient and compressibility. The EOS of CO_2 is then used to calculate the value CO_2 specific volume, at the temperature of interest, which gives the same value of polymer internal pressure. Of all the CO_2 solubility studies listed in Table 6-3, only one value of $\overline{V}_{CO_2}$ is reported. Fleming and Koros[472] give a value of $\overline{V}_{CO_2} = 46.1 \left(cm^3 \middle/ mole \right)$ for CO_2 dissolved in poly(dimethyl siloxane) at T= 35°C and up to a CO_2 mass fraction of 14%. This value was obtained using complementary sorption and dilation data, from which a plot of the total specific volume of the penetrant-laden PMDS as a function of CO_2 mass fraction was generated. The partial specific volumes of the polymer and penetrant (CO_2) were then determined graphically from the tangential slope of the total specific volume versus mass fraction plot. For the same conditions of T and P, and using $T \left(\dfrac{\partial P}{\partial T} \right)_V - P = 2400$ (bar) eqn. (6-8) gives a value of $\overline{V}_{CO_2} = 41.5 \left(cm^3 \middle/ mole \right).$

The proposed method of calculating $\overline{V}_{CO_2}$ by equating the internal pressures of solute and solvent is most accurate for the case of an inert gas dissolved in a non-polar polymer, such as polyethylene, i.e., when solute-solvent interactions are absent. While CO_2 does interact with many polymers, it is suggested that this proposed method does offer the opportunity to incorporate thermodynamic information of the gas and polymer into the value of $\overline{V}_{CO_2}$.

The remainder of this chapter will examine the specific interactions of CO_2 with the three polymers involved in the applications evaluated in this work; poly(methyl methacrylate), PC, and poly(vinyl butyral).

6.1.1 CO_2/PMMA Interactions
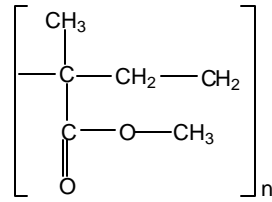
Figure 6-5. *Monomer unit of PMMA.*

Hansen solubility parameter values for PMMA, Figure 6-5, have been determined experimentally by Hansen,[473] and Van Dyk et al.,[474] and calculated by Shaw[475] and Koenhen and Smolders.[476]   As with many commercial polymers, the composition, and therefore the HSP's, will vary between particular manufacturers, and in the case of PMMA a range of HSP values have been determined,

$$d_d = 19.4 - 15.6 \text{ MPa}^{1/2}$$

$$d_p = 10.5 - 5.7 \text{ MPa}^{1/2}$$

$$d_h = 7.8 - 4.7 \text{ MPa}^{1/2}$$

The following average values will be used for this analysis,

$$d_d = d_{dref} = 17.6 \text{ MPa}^{1/2}$$

$$d_d = d_{pref} = 7.1 \text{ MPa}^{1/2}$$

$$d_d = d_{href} = 5.0 \text{ MPa}^{1/2}$$

The interaction radius, Ro (as defined in Section 5.2.1), determined on the basis of PMMA dissolution behavior in a range of liquid solvents is $R_o^{liq} = 8.6$ MPa$^{1/2}$. [477]

Experimental PVT data for PMMA[478] was presented graphically in Figure 5-8. From the PVT data above T_g, indicated by the change in slope of the isobars, the specific volume in the rubber state at ambient conditions, V_{rubber}, is estimated to be $0.8242 \left(cm^3 \middle/ g \right)$, Figure 6.6. This will be taken to be the reference volume of the polymer, V_{ref} at $T_{ref} = 25^\circ$C and $P_{ref} = 1$ bar. From Figure 6.6, the specific volume in the glass state at ambient conditions is $V_{glass} = 0.8460 \left(cm^3 \middle/ g \right)$.
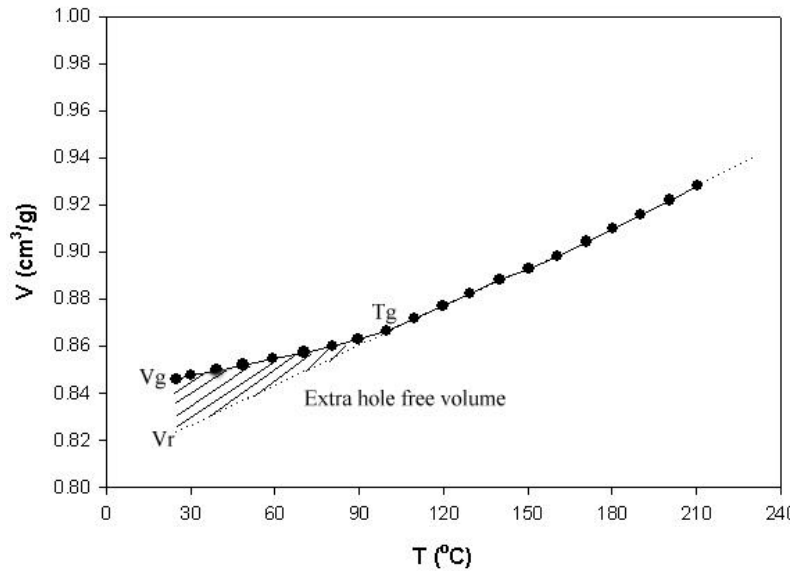
Figure 6-6. *Projected specific volume of PMMA at ambient conditions. The crosshatched region represents the extra volume due to the frozen in "holes" in the glass phase.*

Using the remaining specific volume data for PMMA for $T > T_g$, the change in PMMA volume due to temperature and hydrostatic pressure effects can be determined. As with the specific volume at ambient conditions, V_{rubber}, the specific volume at other

temperatures and pressures below T_g, can be extrapolated from the PVT data above T_g. The change in PMMA specific volume, as a result of temperature and hydrostatic pressure changes are shown in Table 6-6.

Table 6-6. *Change in PMMA specific volume (cm^3/g) as a result of changes in T and P, from PVT data.*[479]

T (°C)	Pressure (bar)			
	0	100	200	400
25	0.0000	-0.0038	-0.0049	-0.0075
30.2	0.0031	-0.0012	-0.0023	-0.0049
39.3	0.0086	0.0033	0.0022	-0.0004
48.7	0.0142	0.0080	0.0069	0.0043
59.5	0.0207	0.0135	0.0124	0.0098
70.4	0.0272	0.0189	0.0178	0.0152
80.6	0.0334	0.0240	0.0229	0.0203
89.7	0.0388	0.0285	0.0275	0.0249
99.8	0.0423	0.0336	0.0325	0.0299
109.8	0.0474	0.0386	0.0375	0.0349
119.8	0.0528	0.0477	0.0425	0.0399
129.6	0.0580	0.0535	0.0489	0.0409
140.1	0.0638	0.0590	0.0542	0.0458
150.5	0.0688	0.0638	0.0588	0.0500

For comparison, this calculation was repeated using the Tait equation, eqns. (5-96), (5-97), and (5-98), and the Tait parameters $A_o = 0.8254 \left(cm^3 / g \right)$, $A_1 = 2.8383 \times 10^{-4} \left(cm^3 / g \cdot {}^\circ C \right)$, $A_2 = 7.792 \times 10^{-7} \left(cm^3 / g \cdot {}^\circ C^2 \right)$, $B_o = 321.59$ *(MPa)*, $B_1 = 4.146 \times 10^{-3} \left(1 / {}^\circ C \right)$, and $C = 0.0894$,[480] as given in Section 5.5.

Table 6-7. *Change in PMMA specific volume (cm^3/g) as a function of changes in T and P, derived from the Tait equation.*

T (°C)	Pressure (bar)			
	0	100	200	400
25	0.0000	-0.0025	-0.0050	-0.0096
30.2	0.0017	-0.0009	-0.0034	-0.0081
39.3	0.0033	0.0007	-0.0019	-0.0067
48.7	0.0048	0.0021	-0.0005	-0.0055
59.5	0.0121	0.0091	0.0063	0.0009
70.4	0.0163	0.0132	0.0102	0.0046
80.6	0.0204	0.0171	0.0140	0.0081
89.7	0.0241	0.0208	0.0175	0.0114
99.8	0.0285	0.0250	0.0216	0.0152
109.8	0.0330	0.0293	0.0257	0.0191
119.8	0.0376	0.0337	0.0300	0.0231
129.6	0.0423	0.0382	0.0344	0.0272
140.1	0.0475	0.0432	0.0392	0.0317
150.5	0.0528	0.0483	0.0441	0.0363

As can be seen from the values in Table 6-6 and Table 6-7, the change in specific volume calculated using the Tait equation are less than that observed from the measured PVT data, but the trend is quite similar.

HSP values for PMMA can also be calculated at different temperatures and pressures using the changes in specific volume given in Table 6-6, and the equations summarized in Table 5-8,

$$\delta_d \ = \ \frac{\delta_{dref}}{\left(\dfrac{V_{ref}}{V^{T,P}}\right)^{-1.25}} \tag{6-9}$$

$$\delta_p = \frac{\delta_{pref}}{\left(\dfrac{V_{ref}}{V^{T,P}}\right)^{-0.5}} \tag{6-10}$$

$$\delta_h = \frac{\delta_{href}}{\exp\left[-1.32 \times 10^{-3}\left(T_{ref} - T\right) - \ln\left(\dfrac{V_{ref}}{V^{T,P}}\right)^{0.5}\right]} \tag{6-11}$$

Table 6-8. *PMMA HSP values (MPa$^{1/2}$), at T and P, calculated using eqns. (6-9)-(6-11).*

T (°C)	Pressure, (bar)											
	0			100			200			400		
	d_l	d_p	d_h	d_l	d_p	d_h	d_l	d_p	d_h	d_l	d_p	d_h
25	17.60	7.10	5.00	17.70	7.12	5.01	17.73	7.12	5.01	17.79	7.13	5.02
30.2	17.52	7.09	4.96	17.63	7.11	4.97	17.66	7.11	4.97	17.72	7.12	4.98
39.3	17.37	7.06	4.88	17.51	7.09	4.90	17.54	7.09	4.90	17.59	7.10	4.91
48.7	17.23	7.04	4.80	17.39	7.07	4.82	17.42	7.07	4.83	17.47	7.08	4.83
59.5	17.06	7.01	4.72	17.25	7.04	4.74	17.28	7.05	4.74	17.33	7.06	4.75
70.4	16.90	6.99	4.63	17.11	7.02	4.66	17.14	7.02	4.66	17.19	7.03	4.66
80.6	16.75	6.96	4.55	16.98	7.00	4.58	17.01	7.00	4.58	17.06	7.01	4.59
89.7	16.62	6.94	4.49	16.87	6.98	4.51	16.89	6.98	4.52	16.94	6.99	4.52
99.8	16.53	6.92	4.42	16.74	6.96	4.44	16.77	6.96	4.44	16.82	6.97	4.45
109.8	16.41	6.90	4.35	16.62	6.94	4.37	16.65	6.94	4.37	16.70	6.95	4.38
119.8	16.29	6.88	4.28	16.41	6.90	4.29	16.53	6.92	4.30	16.67	6.95	4.32
129.6	16.17	6.86	4.21	16.27	6.88	4.22	16.38	6.90	4.23	16.57	6.93	4.25
140.1	16.03	6.84	4.14	16.14	6.86	4.15	16.25	6.88	4.16	16.45	6.91	4.18
150.5	15.92	6.82	4.07	16.03	6.84	4.08	16.15	6.86	4.09	16.35	6.89	4.11

The remaining adjustment to the HSP's of PMMA will be based of the volume change due to CO_2 sorption. From Figure 6-5, PMMA contains a side-chain carbonyl functional group which allows for an acid-base interaction when exposed to CO_2, and from Table 6-3, it can be seen that CO_2 is, in fact, very soluble in PMMA. In Table 6-9, literature values of CO_2 sorption in PMMA, at a variety of temperatures and pressures has been compiled.

Table 6-9. *Literature values of CO₂ sorption in PMMA.*

T (°C)	P (bar)	$[CO_2]$ $\left(cm^3 STP \middle/ cm^3\ polymer \right)$	Ref	T (°C)	P (bar)	$[CO_2]$ $\left(cm^3 STP \middle/ cm^3\ polymer \right)$	Ref
35	13.8	28.04	481	65	30.40	30.94	482
35	27.6	49.71	"	*65*	*37.50*	*38.08*	"
35	*41.4*	*69.74*	"	65	49.60	51.17	"
35	55.2	89.21	"	65	54.70	56.53	"
35	68.9	113.29	"	85	8.80	7.14	"
35	82.7	133.82	"	85	20.30	14.28	"
35	103.4	157.19	"	*85*	*30.40*	*23.80*	"
40	13.5	48.86	483	85	39.20	29.75	"
40	*27.4*	*68.68*	"	85	49.30	39.27	"
40	41.0	84.26	"	*68*	*28.70*	*43.19*	484
40	54.9	101.96	"	68	41.50	58.77	"
40	67.7	119.66	"	68	56.40	75.05	"
40	82.0	152.94	"	68	81.30	110.46	"
40	95.5	170.64	"	68	95.60	118.95	"
35	8.80	17.85	485	68	112.80	125.32	"
35	20.30	39.87	"	68	134.80	143.73	"
35	30.40	56.53	"	68	152.00	167.10	"
35	*39.20*	*77.35*	"	68	172.00	185.51	"
35	49.30	95.20	"	68	192.00	194.71	"
65	8.80	10.71	"	68	217.90	216.66	"
65	22.30	23.80	"	68	253.00	233.66	"

In order to estimate the change in the PMMA specific volume due to CO_2 sorption, it is necessary to evaluate whether the PMMA has been plasticized by the absorbed CO_2, that is, whether T_g of the swollen polymer is above or below the sorption temperature, and therefore whether the dilation can be predicted with the Henry's law relationship, eqn. (6-13). For this evaluation, the experimental data of T_g depression as a function of absorbed CO_2 published by Wissinger *et al.*,[486] and Chiou *et al.* is used,[487] Figure 6-7.
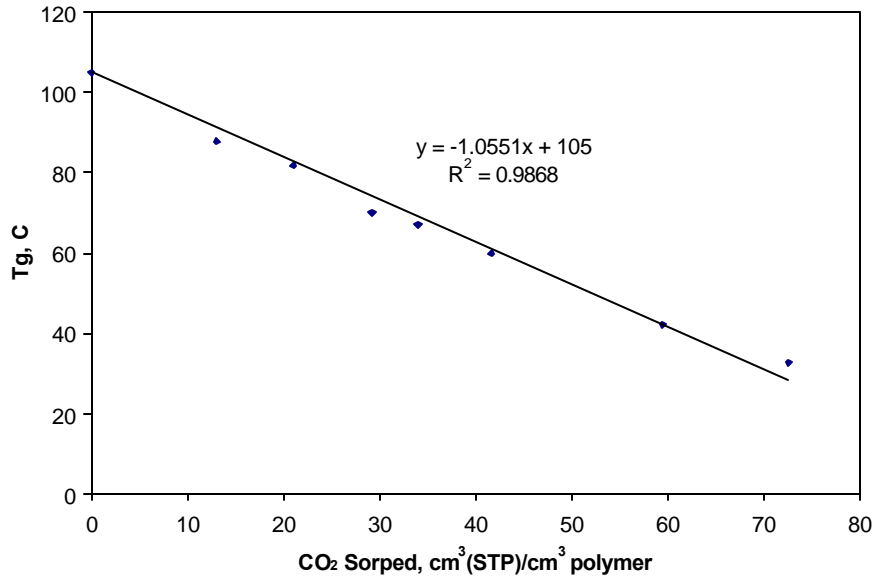
Figure 6-7. *T_g depression in PMMA due to CO_2 sorption.*

From figure 6-7, the depression in T_g as a function of the volume concentration of sorbed CO_2, [CO_2], can be expressed by a linear relation,

$$T_g \left(^\circ C \right) = -1.055 \cdot \left[CO_2 \left(cm^3 \; STP \middle/ cm^3 \; polymer \right) \right] + 105 \qquad (6\text{-}12)$$

the experimental PMMA sorption data given in Table 6-9 was evaluated, using this linear relation, to determine where the transition from the glass to rubber state occurs, i.e., which values of T are above T_g at each value of P. This transition has been indicated for the respective data sets in Table 6-9 by the bold, italic type. Using the sorption data in Table 6-9, where the polymer is in the rubber phase, a correlation was developed, eqn. (6-13), for the sorption of CO_2 versus temperature as a function of pressure, shown in Figure 6-8.
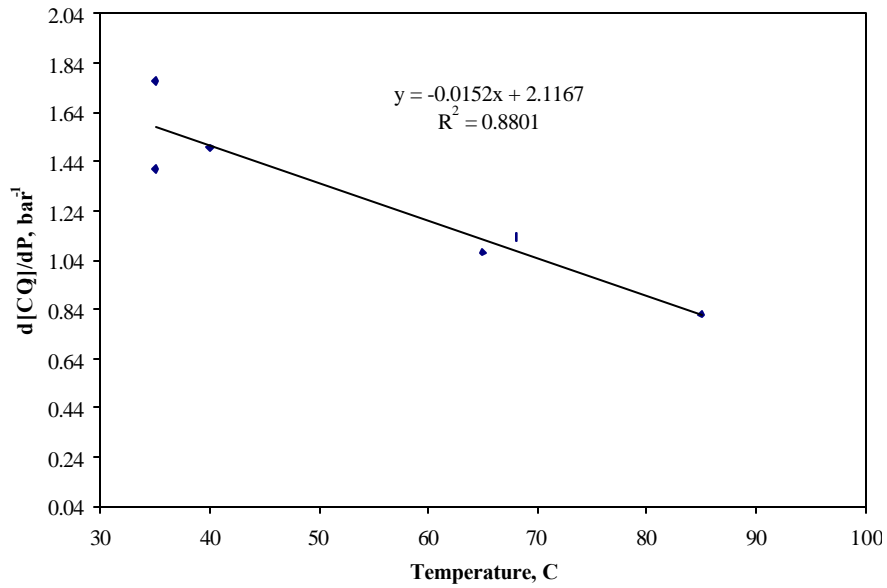
Figure 6-8. *CO_2 sorption, [CO_2], in PMMA as a function of pressure versus temperature.*

With this relationship,

$$[CO_2]\left(\frac{cm^3\ STP}{cm^3\ polymer}\right) = \left(-\,0.0152\cdot T(^\circ C) + 2.1167\right)P\,(bar) \qquad (6\text{-}13)$$

and using eqn. (6-7), the following correlation can be made for the volume dilation of PMMA swelled by CO_2

6-149

$$\frac{\Delta V^{CO_2}}{V_{Polymer}^0} = k_D P \cdot \left(\frac{\overline{V}_{CO_2}}{22415}\right) = [CO_2]\left(\frac{\overline{V}_{CO_2}}{22415}\right) \tag{6-14}$$

The partial molar volumes of CO_2 dissolved in PMMA are calculated using the method outlined in the previous section, eqn. (6-8). The results for the temperature and pressure range of interest, are presented in Table 6-10.

Table 6-10. *Calculated CO_2 partial molar volumes in PMMA.*

T, (^{o}C)	P, (bar)	Internal Pressure, PMMA (bar)	$\overline{V}_{CO_2}\left(cm^3/mol\right)$
35	100	3833.8	39.6
35	200	3845.5	39.4
50	100	3767.5	40.2
50	200	3779.1	39.8
100	100	3530.6	42.6
100	200	3541.9	42.2
Average			40.6

Therefore,

$$\frac{\Delta V^{CO_2}}{V_{Polymer}^0} = (-0.017T + 2.164)P\left(\frac{\overline{V}^{CO_2}}{22415}\right) \tag{6-15}$$

where a value of $\overline{V}_{CO_2} = 40.6 \left(cm^3/mole\right)$ is used, as determined in Table 6-10. Equation (6-15) has been used to calculate the volume change of PMMA due to CO_2 sorption, and the results are given in Table 6-11. Values above 35^oC and 39 bar have been approximated, where the earliest transition occurred in the experimental data and up to 200 bar due to unknown hydrostatic pressure effects above the experimental values in Table 6-11.

Table 6-11. *Change in PMMA specific volume* $\left(cm^3\!\!\big/_{mole}\right)$ *due to of CO_2 swelling.*

	Pressure (bar)	
T (°C)	100	200
25	—	—
30.2	—	—
39.3	0.2231	0.4461
48.7	0.1992	0.3985
59.5	0.1719	0.3437
70.4	0.1442	0.2885
80.6	0.1184	0.2367
89.7	0.0953	0.1906
99.8	0.0697	0.1394
109.8	0.0443	0.0887
119.8	0.0190	0.0380

With the data in Table 6-11, the solubility parameters of PMMA can be adjusted for T, P, and CO_2 swelling, with the results given in Table 6-12.

Table 6-12. *PMMA HSP's ($MPa^{1/2}$) adjusted for the effects of T, P, and dilation due to CO_2 sorption.*

	Pressure (bar)								
	0			100			200		
T (°C)	d_d	d_p	d_h	d_d	d_p	d_h	d_d	d_p	d_h
25	17.60	7.10	5.00	17.70	7.12	5.01	17.73	7.12	5.01
30.2	17.52	7.09	4.96	17.63	7.11	4.97	17.66	7.11	4.97
39.3	17.37	7.06	4.88	12.99	6.29	4.35	10.23	5.71	3.95
48.7	17.23	7.04	4.80	13.30	6.35	4.33	10.67	5.81	3.97
59.5	17.06	7.01	4.72	13.66	6.42	4.32	11.24	5.93	3.99
70.4	16.90	6.99	4.63	14.04	6.49	4.30	11.86	6.06	4.02
80.6	16.75	6.96	4.55	14.42	6.56	4.29	12.50	6.19	4.05
89.7	16.62	6.94	4.49	14.77	6.62	4.28	13.12	6.31	4.08
99.8	16.53	6.92	4.42	15.18	6.69	4.27	13.89	6.46	4.12
109.8	16.41	6.90	4.35	15.61	6.77	4.26	14.73	6.61	4.16
119.8	16.29	6.88	4.28	15.97	6.83	4.24	15.66	6.78	4.21

From Table 6-12, the effect of swelling due to CO_2 sorption has a significant impact on the PMMA solubility parameters, and especially the dispersion parameter, d_d, which, as discussed in Section 3-1, varies rapidly with intermolecular distance. The

calculated HSP initially decrease with temperature along an isobar, but then begin to increase with temperature. This is due to the combination of lower CO_2 density and the effect of hydrostatic pressure on the free volume of the polymer, as discussed in Section 6.1.

6.1.2 CO_2/PC Interactions
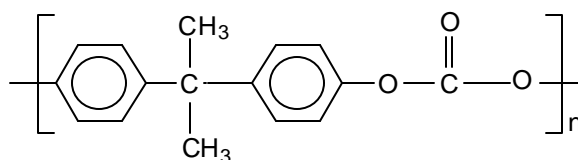
Figure 6-9.   *Structural repeat unit of Polycarbonate.*

Total solubility parameter values for polycarbonate (PC) are available from several sources. The total solubility parameters and the associated reference are given below,

$$d_T = 21 \text{ MPa}^{1/2} \text{ } [488]$$
$$d_T = 19.6 \text{ MPa}^{1/2} \text{ } [489]$$
$$d_T = 19 - 22 \text{ MPa}^{1/2} \text{ } [490]$$
$$d_T = 19.4 - 21.7 \text{ MPa}^{1/2} \text{ } [491]$$

HSP's, for PC have been determined experimentally by Hansen,[492] and these values will be used for this analysis,

$$d_d = 18.1 \text{ MPa}^{1/2}$$
$$d_p = 5.9 \text{ MPa}^{1/2}$$
$$d_h = 6.9 \text{ MPa}^{1/2}$$

The interaction radius, *Ro* (as defined in Section 5.2.1), determined on the basis of PC dissolution behavior in a range of liquid solvents is $R_o^{liq} = 5.5 \text{ MPa}^{1/2}$. [493]

Experimental PVT data for PC[494] was presented graphically in Figure 5-10. From the PVT data above T_g, indicated by the change in slope of the isobars, the specific volume in the rubber state at ambient conditions, V_{rubber}, is estimated to be $0.7947 \left(\frac{cm^3}{g} \right)$, Figure 6-10, and will be used as the reference volume, V_{ref}, at $T_{ref} = 25°C$ and $P_{ref} = 1$ bar. The glass state specific volume at ambient conditions is $V_{glass}, = 0.8418 \left(\frac{cm^3}{g} \right)$.
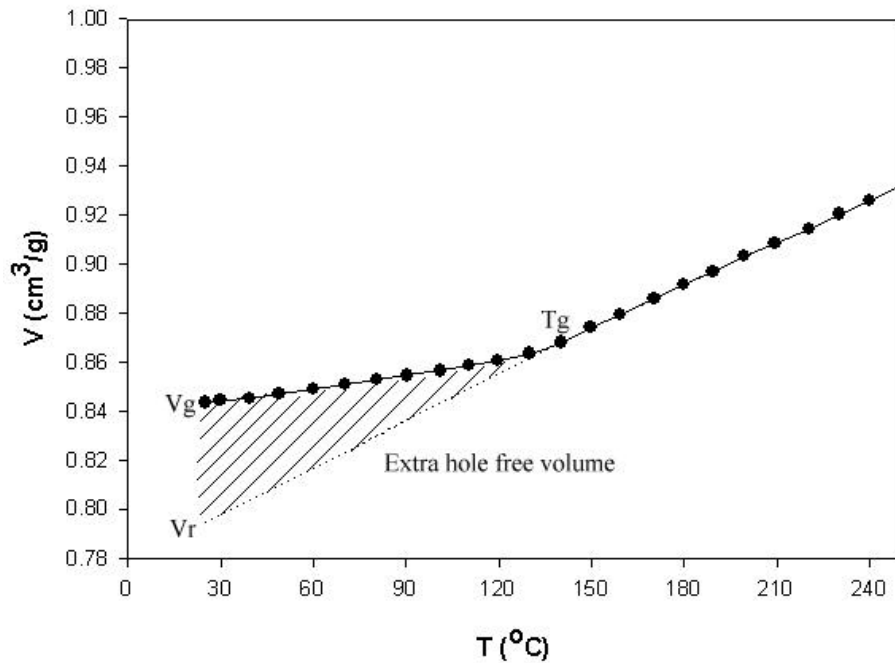
Figure 6-10. *Projected specific volume of PC at ambient conditions.*

The experimental specific volume data for $T > T_g$, a can be used to determine the change in PC volume due to temperature and hydrostatic pressure effects. As with the rubber-state specific volume at ambient conditions, V_{rubber}, the specific volume at other temperatures and pressures below T_g can be extrapolated from the PVT data above T_g.

The calculated change in PC specific volume, as a result of temperature and hydrostatic pressure changes are given in Table 6-13

Table 6-13. *Change in PC specific volume* $\left(cm^3 \middle/ g \right)$ *as a result of changes in T and P, derived from the experimental PVT data.*[495]

T (°C)	Pressure (bar)			
	0	100	200	400
25	0.0000	0.0035	-0.0005	-0.0011
30	0.0030	0.0091	0.0020	0.0014
39.3	0.0086	0.0149	0.0066	0.0061
49	0.0144	0.0155	0.0115	0.0109
59.9	0.0209	0.0214	0.0170	0.0164
70.2	0.0271	0.0276	0.0221	0.0215
80.7	0.0334	0.0339	0.0274	0.0268
90.4	0.0392	0.0397	0.0322	0.0316
101	0.0456	0.0461	0.0375	0.0369
110.6	0.0514	0.0519	0.0423	0.0417
119.8	0.0569	0.0574	0.0469	0.0463
130	0.0630	0.0635	0.0520	0.0514
140.1	0.0691	0.0696	0.0571	0.0565
149.8	0.0794	0.0754	0.0619	0.0613
159.4	0.0848	0.0845	0.0667	0.0661
170.3	0.0912	0.0852	0.0791	0.0716
179.7	0.0969	0.0906	0.0843	0.0744
189.3	0.1024	0.0959	0.0893	0.0790

This calculation was repeated using the Tait equation, eqn. (5-96), (5-97), and (5-98), and the Tait parameters[496] $A_0 = 0.7917 \left(cm^3 \middle/ g \right)$, $A_1 = 4.4201 \times 10^{-4} \left(cm^3 \middle/ g \cdot °C \right)$, $A_2 = 2.8583 \times 10^{-7} \left(cm^3 \middle/ g \cdot °C^2 \right)$, $B_0 = 312.7 \ (MPa)$, $B_1 = 3.9728 \times 10^{-3} \left(1 \middle/ °C \right)$, and C = 0.0894, as discussed in Section 5.5.

Table 6-14. *Change in PC specific volume (cm^3/g) as a function of change in T and P, derived from the Tait equation.*

T (°C)	Pressure (bar_			
	0	100	200	400
25	0.0000	-0.0025	-0.0049	-0.0095
30	0.0023	-0.0003	-0.0027	-0.0074
39.3	0.0066	0.0039	0.0014	-0.0035
49	0.0111	0.0083	0.0057	0.0006
59.9	0.0116	0.0088	0.0061	0.0010
70.2	0.0163	0.0134	0.0106	0.0053
80.7	0.0212	0.0182	0.0152	0.0097
90.4	0.0263	0.0231	0.0200	0.0143
101	0.0311	0.0277	0.0245	0.0185
110.6	0.0363	0.0328	0.0295	0.0232
119.8	0.0412	0.0375	0.0340	0.0275
130	0.0458	0.0420	0.0384	0.0316
140.1	0.0511	0.0471	0.0433	0.0362
149.8	0.0563	0.0521	0.0482	0.0408
159.4	0.0614	0.0570	0.0529	0.0453
170.3	0.0665	0.0619	0.0576	0.0497
179.7	0.0723	0.0676	0.0631	0.0548
189.3	0.0774	0.0725	0.0678	0.0592

As was found for PMMA, the changes in PC specific volume calculated with the Tait equation are less than the measured PVT data, but the trend is preserved.

HSP values for PC, as a function of T and hydrostatic pressure, can also be calculated using the changes in specific volume, along with the equations summarized in Table 5-9. The results are given in Table 6-15.

Table 6-15. *PC HSP values (MPa$^{1/2}$), at T and P, calculated using eqns. (6-9)-(6-11).*

T (°C)	Pressure (bar)											
	0			100			200			400		
	δ_d	δ_p	δ_h	δ_d	δ_p	δ_h	δ_d	δ_p	δ_h	δ_d	δ_p	δ_h
25	18.10	5.90	6.90	18.09	5.90	6.94	18.11	5.90	7.07	18.13	5.90	7.07
30	18.01	5.89	6.84	18.00	5.89	6.93	18.04	5.89	7.06	18.06	5.89	7.06
39.3	17.86	5.87	6.73	17.84	5.87	6.91	17.91	5.88	7.04	17.93	5.88	7.04
49	17.70	5.85	6.63	17.68	5.85	6.88	17.78	5.86	7.02	17.79	5.86	7.02
59.9	17.52	5.82	6.50	17.51	5.82	6.86	17.63	5.84	7.00	17.65	5.84	6.99
70.2	17.36	5.80	6.39	17.34	5.80	6.83	17.49	5.82	6.98	17.51	5.82	6.97
80.7	17.19	5.78	6.28	17.18	5.78	6.81	17.35	5.80	6.95	17.37	5.80	6.95
90.4	17.04	5.76	6.18	17.03	5.76	6.79	17.22	5.78	6.93	17.24	5.79	6.93
101	16.88	5.74	6.07	16.87	5.74	6.76	17.09	5.77	6.91	17.10	5.77	6.91
110.6	16.74	5.72	5.97	16.72	5.72	6.74	16.96	5.75	6.89	16.98	5.75	6.89
119.8	16.60	5.70	5.88	16.59	5.70	6.72	16.85	5.73	6.88	16.86	5.74	6.87
130	16.45	5.68	5.78	16.44	5.68	6.70	16.72	5.72	6.86	16.74	5.72	6.85
140.1	16.31	5.66	5.69	16.30	5.66	6.68	16.60	5.70	6.84	16.61	5.70	6.83
149.8	16.07	5.63	5.58	16.16	5.64	6.66	16.48	5.68	6.82	16.49	5.68	6.81
159.4	15.95	5.61	5.49	15.95	5.61	6.62	16.37	5.67	6.80	16.38	5.67	6.79
170.3	15.80	5.59	5.39	15.94	5.61	6.62	16.08	5.63	6.75	16.25	5.65	6.77
179.7	15.68	5.57	5.31	15.82	5.59	6.60	15.96	5.61	6.73	16.18	5.64	6.76
189.3	15.56	5.55	5.23	15.70	5.57	6.58	15.84	5.59	6.72	16.08	5.63	6.74

The remaining adjustment to the PC solubility parameter values will be based on the volume change due to CO_2 sorption. As can be seen from Figure 6-8, PC contains a main-chain carbonyl functional group, which allows for an acid-base interaction when exposed to CO_2, and from Table 6-3, it can be seen that CO_2 is slightly soluble in PC. Table 6-16 is a compilation of literature values of CO_2 solubility in PC.

Table 6-16. *Literature values of CO$_2$ solubility in PC.*

T (°C)	P (bar)	[CO$_2$] $\left(cm^3 STP / cm^3\ polymer \right)$	Ref	T (°C)	P (bar)	[CO$_2$] $\left(cm^3 STP / cm^3\ polymer \right)$	Ref	T (°C)	P (bar)	[CO$_2$] $\left(cm^3 STP / cm^3\ polymer \right)$	Ref
35	10.8	15.6	497	35	13.1	12.50	498	75	4.75	4.50	499
35	25.3	32.88	"	35	26.3	37.50	"	75	6	5.00	"
35	41.6	48	"	35	42.1	46.70	"	75	7.3	6.50	"
35	59	61.56	"	35	50	50.00	"	75	9	6.75	"
35	76	70.8	"	35	71	58.30	"	75	10	8.25	"
35	95	73.2	"	35	97.4	**77.50**	"	75	11.8	8.50	"
35	13.8	26.26	500	35	128.9	81.70	"	75	13	9.50	"
35	20.7	34.50	"	35	171.1	85.00	"	75	14.5	10.00	"
35	27.6	40.50	"	35	215.8	86.70	"	75	16	11.00	"
35	34.5	49.50	"	55	1.84	4.55	501	75	18	11.50	"
35	41.4	54.00	"	55	2.76	6.36	"	100	4.75	2.50	"
35	48.3	60.00	"	55	4.6	8.20	"	100	6	3.40	"
35	55.2	66.00	"	55	8.3	11.80	"	100	7.3	4.00	"
35	62.1	73.50	"	55	12.9	15.50	"	100	9	4.70	"
40	13.5	36.00	502	55	20.3	20.90	"	100	10	5.50	"
40	27.4	51.00	"	55	30.4	26.40	"	100	11.8	6.00	"
40	41	51.00	"	55	37.3	30.00	"	100	13	6.50	"
40	54.9	66.00	"	55	44.2	31.80	"	100	14.5	7.00	"
40	67.7	63.00	"	55	49.7	34.50	"	100	16	7.50	"
40	82	60.00	"					100	18	8.00	"
40	95.5	**81.00**	"								

Estimating the change in PC specific volume resulting from CO_2 swelling again requires finding a relationship between T_g and concentration of sorbed CO_2. Sorption data above T_g can then be evaluated with the Henry's law relationship to generate changes in polymer specific volume. For this evaluation, reported T_g depression data for PC as a function of sorbed CO_2,[503] is plotted in Figure 6-11.
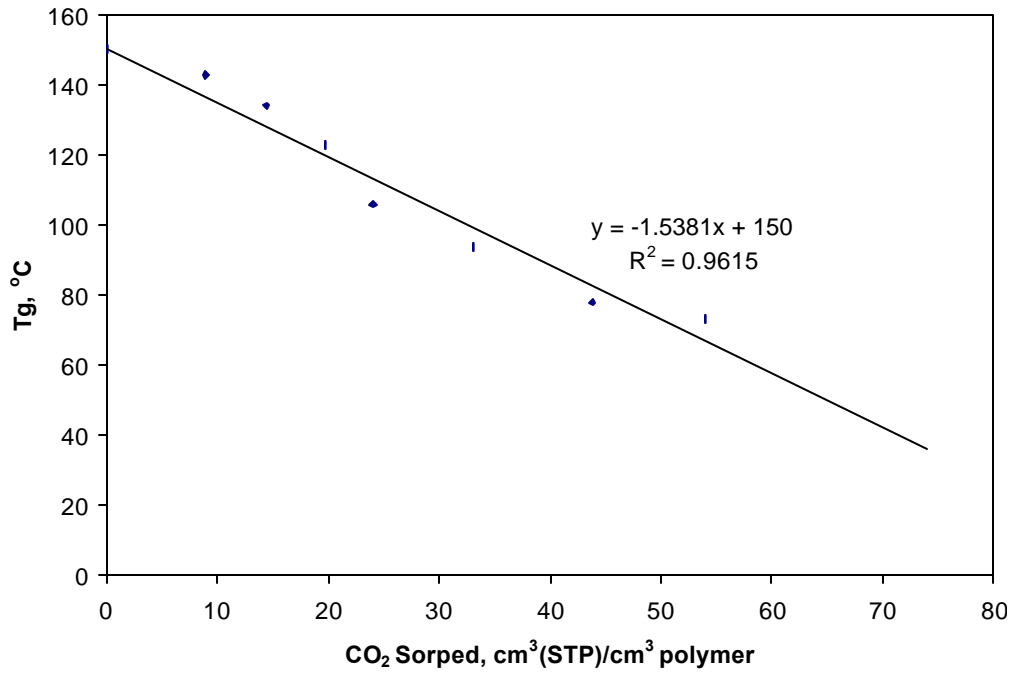
Figure 6-11. T_g depression in PC due to CO_2 sorption.

As shown in Figure 6-11, the T_g depression due to CO_2 sorption can be expressed by a linear relation,

$$T_g(^\circ C) = -1.5381 \cdot \left[CO_2 \left(\frac{cm^3 \, STP}{cm^3 \, polymer} \right) \right] + 150 \qquad (6\text{-}16)$$

The experimental PC sorption data in Table 6-16 was evaluated, using this linear relation, to determine the conditions of T and P for the glass to rubber transition. This transition

has been indicated for the respective data sets in Table 6-17 with bold, italic type. In contrast to the tabulated, experimental PMMA data, Table 6-X, only two glass to rubber transitions are predicted to occur in the tabulated PC data. This is explained by the higher (ambient condition) glass transition temperature for PC, and the lower CO_2 solubility, as compared to PMMA, as well as the fact that only one PC sorption study was performed at sufficiently high pressures. As a result, an alternative approach will be used to estimate the CO_2 sorption effect on the PC HSP's.

Von Schnitzler et al.,[504] has measured PC volume swelling at temperatures ranging from 40 to 120°C and at 100 and 300 bar. Their data are plotted in Figure 6-12.
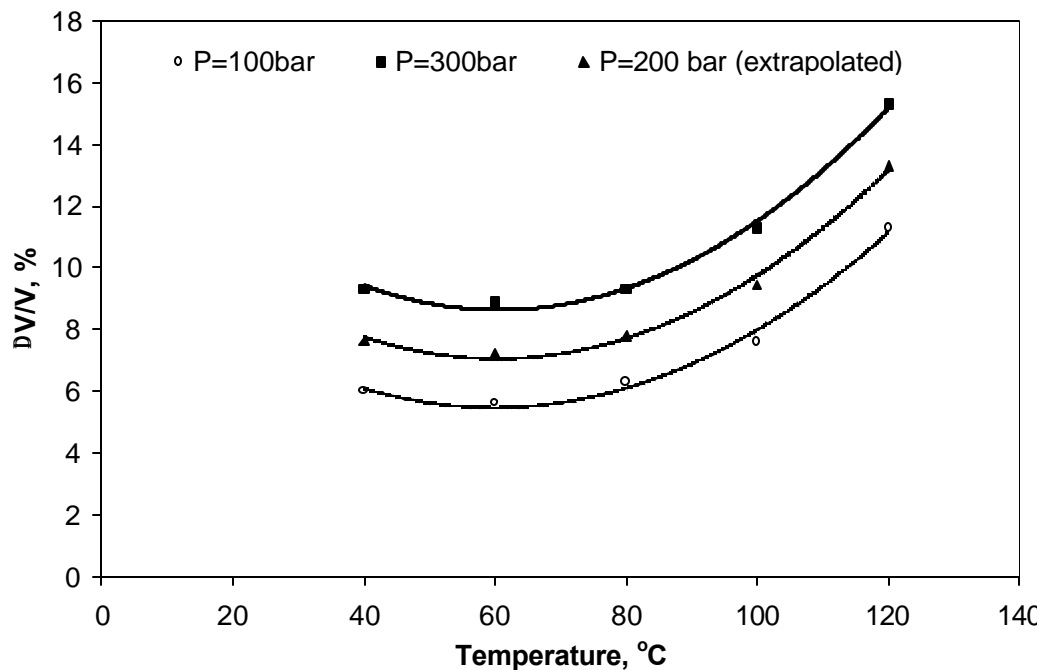
Figure 6-12. *Experimental measurements of PC swelling due to CO_2 sorption (lines drawn based on fit with experimental data).*

From Figure 6-12, it appears that the PC swelling behavior is approximately linear above 80°C along each of the isobars, and the swelling behavior is expressed as

(At 100 bar) $$\frac{\Delta V^{CO_2}}{V_{Polymer}^0} = 0.0013T - 0.041 \qquad (6\text{-}17)$$

(At 200 bar) $$\frac{\Delta V^{CO_2}}{V_{Polymer}^0} = 0.00138T - 0.0357 \qquad (6\text{-}18)$$

(At 300 bar) $$\frac{\Delta V^{CO_2}}{V_{Polymer}^0} = 0.0015T - 0.00333 \qquad (6\text{-}19)$$

The CO_2 sorption which corresponds to these swelling isobars can be determined with eqn. (6-7) and the CO_2 partial molar volume in PC. As with PMMA, the CO_2 partial molar volumes in PC are calculated using the assumption stated in eqn. (6-8), PC PVT data, and the CO_2 EOS (eqn. 5-14). Results, for the temperature and pressure range of interest here, are presented in Table 6-17.

Table 6-17. *Calculated partial molar volumes of CO_2 dissolved in PC.*

T (^{o}C)	P (bar)	Internal Pressure, PC (bar)	$\overline{V}_{CO_2} \left(cm^3/mol \right)$
50	100	3936.3	39.6
50	200	3972.1	39.1
100	100	3545.7	42.6
100	200	3713.3	41.5
Average			40.7

Rearranging eqn. (6-7), the CO_2 sorption can be now be calculated using,

$$[CO_2] = \frac{\Delta V^{CO_2}}{V_{Polymer}^0} \cdot \left(\frac{22415}{\overline{V}_{CO_2}} \right) \qquad (6\text{-}20)$$

where an average value of 40.7 $\left(cm^3/mol \right)$ is used for $\overline{V}_{CO_2}$, Table 6-17. The swelling data in Figure 6-12, for $T \geq 80^oC$, are shown in Table 6-18, along with the CO_2 volume

fraction calculated from eqn. (6-20), and the glass transition temperature from eqn. (6-16) with the $[CO_2]$ result of eqn. (6-20).

Table 6-18. *Calculated CO_2 sorption and T_g depression for PC.*

T (^{o}C)	P (bar)	$\Delta V/V$	$[CO_2]$ $\left(cm^3 \ STP \middle/ cm^3 polymer \right)$	T_g (^{o}C)
80	100	0.063	34.7	96.6
100	100	0.076	41.9	85.6
120	100	0.113	62.2	54.3
80	300	0.093	51.2	71.2
100	300	0.113	62.2	54.3
120	300	0.153	84.3	20.4

The results of Table 6-18 appear reasonable based on the data shown in Figure 6-12. At 300 bar and 80°C, the swelling behavior appears to transition to a linear behavior and from Table 6-18, the predicted CO_2 sorption indicates a transition temperature of 71.2°C. At 100 bar and 80°C, the polymer has softened and by 100°C is predicted to have passed through a depressed transition temperature.

The change in PC specific volume due to CO_2 sorption is shown in Table 6-19. Equations (6-17) and (6-18) were used to calculate the PC volume changes at temperatures greater than or equal to 80°C, and for the temperature range 40°C to 79°C, $\left(\Delta V^{CO_2} \middle/ V^o_{Polymer} \right)$ is estimated to be 0.056 at 100 bar and 0.073 at 200 bar, based on the data in Figure 6-12.

Table 6-19. *Change in PC specific volume,* $\left(cm^3/mol\right)$, *as a result of CO_2 swelling.*

T (°C)	Pressure (bar) 100	200	300
25			
30			
39.3	0.0445	0.0580	0.0707
49	0.0445	0.0580	0.0707
59.9	0.0445	0.0580	0.0707
70.2	0.0445	0.0580	0.0707
80.7	0.0476	0.0580	0.0721
90.4	0.0572	0.0704	0.0837
101	0.0677	0.0820	0.0963
110.6	0.0773	0.0925	0.1077
119.8	0.0864	0.1026	0.1187
130	0.0966	0.1137	0.1309
140.1	0.1066	0.1247	0.1429
149.8	0.1162	0.1353	0.1545
159.4	0.1258	0.1458	0.1659

The PC HSP's can now be adjusted for the effects of T, P, and CO_2 dilation, with the results given in Table 6-20.

Table 6-20. *PC HSP values $(MPa^{1/2})$ adjusted for T, P, and CO_2 swelling.*

T (°C)	Pressure (bar) 0 d_d	d_p	d_h	100 d_d	d_p	d_h	200 d_d	d_p	d_h	300 d_d	d_p	d_h
25	18.10	5.90	6.90	18.11	5.90	6.90	18.11	5.90	7.07	18.13	5.90	7.07
30	18.01	5.89	6.84	18.03	5.89	6.84	18.04	5.89	7.06	18.06	5.89	7.06
39.3	17.86	5.87	6.73	16.03	5.62	6.45	16.41	5.67	6.80	16.13	5.63	6.75
49	17.70	5.85	6.63	15.91	5.60	6.35	16.30	5.66	6.78	16.02	5.62	6.73
59.9	17.52	5.82	6.50	15.77	5.58	6.24	16.17	5.64	6.76	15.89	5.60	6.71
70.2	17.36	5.80	6.39	15.65	5.57	6.13	16.05	5.62	6.74	15.78	5.58	6.69
80.7	17.19	5.78	6.28	15.32	5.52	6.00	15.66	5.57	6.67	15.63	5.56	6.67
90.4	17.04	5.76	6.18	14.90	5.46	5.86	15.30	5.52	6.61	15.28	5.51	6.61
101	16.88	5.74	6.07	14.48	5.40	5.71	14.98	5.47	6.56	14.91	5.46	6.54
110.6	16.74	5.72	5.97	14.11	5.34	5.58	14.68	5.43	6.51	14.59	5.41	6.49
119.8	16.60	5.70	5.88	13.85	5.30	5.47	14.59	5.41	6.49	14.30	5.37	6.43
130	16.45	5.68	5.78	13.49	5.24	5.34	14.28	5.37	6.44	13.98	5.32	6.38
140.1	16.31	5.66	5.69	13.14	5.19	5.21	13.99	5.32	6.39	13.68	5.28	6.32
149.8	16.07	5.63	5.58	12.79	5.13	5.09	13.72	5.28	6.34	13.40	5.23	6.27

Once again, the sorption of CO_2 and resultant swelling of the PC results in a decrease in the polymer's HSP values, with the largest decrease observed in the dispersion parameter, d_d. Unlike PMMA, however, the HSP values for PC continue to decrease with increasing temperature, indicating a continuous uptake of CO_2.

6.1.3 CO_2/PVB Interactions
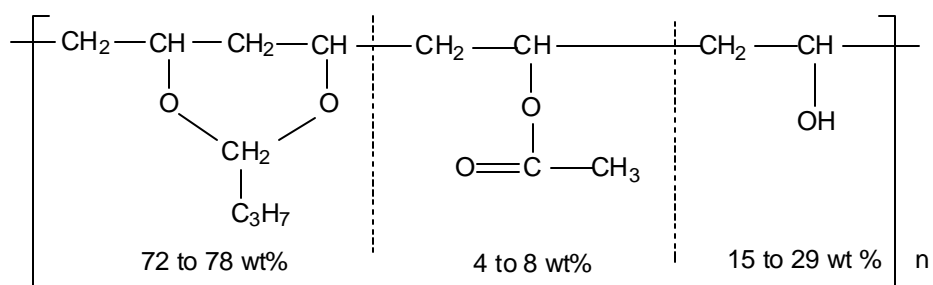
Figure 6-13. Monomer structure of PVB showing the typical range of composition.

Poly(vinyl butyral), Figure 6-13, is a polymer manufactured from poly(vinyl alcohol) by polymerizing butyl aldehyde.   In the chemical reaction, 100% butyralization does not take place, resulting in a considerable amount of residual hydroxyl (vinyl alcohol), from 15 to 29 wt.%, in the PVB.   There is also a small amount of residual acetyl (4 to 8 wt. %).   As a result, the properties of this polymer will vary based upon the overall polymer composition.   In solution or in the solid form this polymer tends to hydrogen bond internally, so solubility is dependent on an appreciable acid-base interaction with basic solvents.

HSP solubility parameter values are available from a variety of sources.   Two sets of HSP values for Butvar® B76-poly(vinyl butyral) (11-13 wt.% hydroxyl), manufactured by Shawinigan Resins Company have been reported,

$$\text{Set 1}[505] \quad \begin{aligned} d_d &= 17.4 \text{ MPa}^{1/2} \\ d_p &= 8.8 \text{ MPa}^{1/2} \\ d_h &= 11.3 \text{ MPa}^{1/2} \end{aligned}$$

$$\text{Set 2}[506] \quad \begin{aligned} d_d &= 18.6 \text{ MPa}^{1/2} \\ d_p &= 4.4 \text{ MPa}^{1/2} \\ d_h &= 13.1 \text{ MPa}^{1/2} \end{aligned}$$

Using the group contribution method, Sincock and David[507] determined HSP values, assuming a 28 wt.% hydroxyl content and 72 wt.% vinyl butyral,

$$\begin{aligned} d_d &= 15.7 \text{ MPa}^{1/2} \\ d_p &= 8.2 \text{ MPa}^{1/2} \\ d_h &= 11.4 \text{ MPa}^{1/2} \end{aligned}$$

HSP values calculated with the PVB weight percents specified in the Sekisui Materials Safety Data Sheet for the poly(vinyl butyral) product S-Lec B (72 wt.% vinyl butyral, 4 wt.% acetyl, and 24 wt.% hydroxyl) are

$$\begin{aligned} d_d &= 15.3 \text{ MPa}^{1/2} \\ d_p &= 6.6 \text{ MPa}^{1/2} \\ d_h &= 9.4 \text{ MPa}^{1/2} \end{aligned}$$

An averaged set of HSP's and an interaction radius as determined by Hansen,[508] will be used:

$$\begin{aligned} d_d &= d_{dref} = 16.8 \text{ MPa}^{1/2} \\ d_d &= d_{pref} = 7.0 \text{ MPa}^{1/2} \\ d_d &= d_{href} = 11.3 \text{ MPa}^{1/2} \end{aligned}$$

The interaction radius, Ro (as defined in Section 5.2.1), determined on the basis of PVB dissolution behavior in a range of liquid solvents is $R_o^{liq} = 9.8 \text{ MPa}^{1/2}$.[509]

Experimental PVT data for PVB[510] are presented graphically in Figure 5-9. From these data, noticeable 'dips' can be observed along the isobars at higher pressures. This

is a feature occasionally observed in polymer PVT data, and is due to nonequilibrium states belonging to different glasses formed under different conditions during the measurement cycle. The glasses formed in this region are generally formed at pressures higher then the formation pressure of the "initial" glass, and therefore may have a higher density than the initial glass. This lead to the pronounced 'dips' (densifications) in the plotted isobars.[511] From the PVT data above T_g, indicated by the change in slope of the isobars, the specific volume in the rubber state at ambient conditions, V_{rubber}, is estimated to be $0.9074 \left(cm^3 / g \right)$, Figure 6-14, and will be taken as the reference volume, V_{ref}, at $T_{ref} = 25^o C$ and $P_{ref} = 1$ bar. The glass state specific volume at ambient conditions is $V_{glass} = 0.9171 \left(cm^3 / g \right)$.
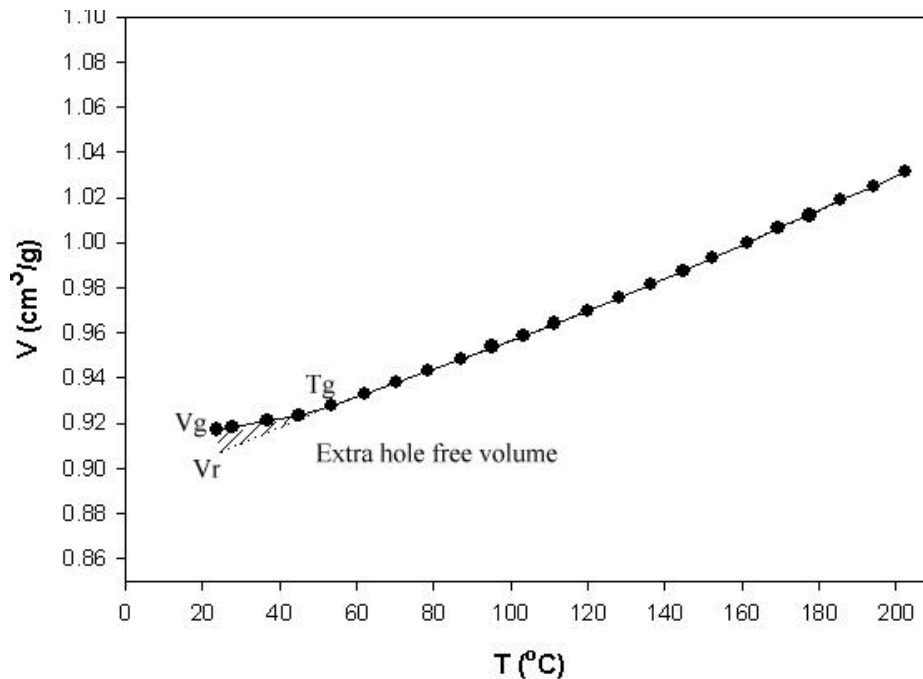
Figure 6-14. *Extrapolation of the specific volume of PVB in the rubber state to ambient conditions.*

With the remaining specific volume data for PVB above Tg, the change in PVB volume due to temperature and hydrostatic pressure effects can be determined, and the results are given in Table 6-21.

Table 6-21. *Change in PVB specific volume (cm^3/g) as a result of T and P changes, derived from PVT data.*

T (^{o}C)	Pressure (bar)			
	0	100	200	300
25	0.0000	-0.0036	-0.0073	-0.0114
27.8	0.0020	-0.0016	-0.0056	-0.0097
36.9	0.0083	0.0047	-0.0002	-0.0043
45.1	0.0141	0.0105	0.0048	0.0007
53.4	0.0204	0.0163	0.0097	0.0056
62	0.0256	0.0212	0.0168	0.0108
70.2	0.0309	0.0261	0.0212	0.0157
78.6	0.0359	0.0309	0.0259	0.0215
87.1	0.0410	0.0357	0.0304	0.0258
95.2	0.0464	0.0409	0.0353	0.0306
103.4	0.0513	0.0456	0.0398	0.0349
111.3	0.0567	0.0507	0.0447	0.0396
119.9	0.0624	0.0562	0.0499	0.0446
128.2	0.0681	0.0615	0.0548	0.0493
136.4	0.0739	0.0671	0.0602	0.0545
144.8	0.0799	0.0728	0.0656	0.0597
152.3	0.0855	0.0782	0.0709	0.0648
161.3	0.0926	0.0847	0.0767	0.0703

No Tait parameters have been published for PVB so that a comparison between the volume changes determined from experimental PVT data and calculated using the Tait equation cannot be made.

HSP values for PVB are calculated at different temperatures and pressures using the calculated changes in specific volume and the equations summarized in Table 5-9 are given in Table 6-22.

Table 6-22. *PVB HSP values (MPa$^{1/2}$), at T and P, calculated using eqns. (6-9)-(6-11).*

T (^{o}C)	Pressure (bar)											
	0			100			200			300		
	d_d	d_p	d_h	d_d	d_p	d_h	d_d	d_p	d_h	d_d	d_p	d_h
25	16.8	7.0	11.3	16.9	7.0	11.5	17.0	7.0	11.5	17.1	7.0	11.6
27.8	16.8	7.0	11.2	16.8	7.0	11.5	16.9	7.0	11.5	17.0	7.0	11.6
36.9	16.6	7.0	11.1	16.7	7.0	11.5	16.8	7.0	11.5	16.9	7.0	11.5
45.1	16.5	6.9	10.9	16.6	7.0	11.4	16.7	7.0	11.5	16.8	7.0	11.5
53.4	16.3	6.9	10.8	16.4	6.9	11.4	16.6	7.0	11.4	16.7	7.0	11.5
62	16.2	6.9	10.6	16.3	6.9	11.4	16.4	6.9	11.4	16.6	7.0	11.4
70.2	16.1	6.9	10.5	16.2	6.9	11.4	16.3	6.9	11.4	16.4	6.9	11.4
78.6	16.0	6.9	10.3	16.1	6.9	11.3	16.2	6.9	11.3	16.3	6.9	11.4
87.1	15.9	6.8	10.2	16.0	6.9	11.3	16.1	6.9	11.3	16.2	6.9	11.3
95.2	15.8	6.8	10.0	15.9	6.8	11.3	16.0	6.9	11.3	16.1	6.9	11.3
103.4	15.7	6.8	9.9	15.8	6.8	11.2	15.9	6.9	11.3	16.0	6.9	11.3
111.3	15.6	6.8	9.8	15.7	6.8	11.2	15.8	6.8	11.2	15.9	6.9	11.3
119.9	15.5	6.8	9.6	15.6	6.8	11.2	15.7	6.8	11.2	15.8	6.8	11.2
128.2	15.3	6.8	9.5	15.5	6.8	11.2	15.6	6.8	11.2	15.7	6.8	11.2
136.4	15.2	6.7	9.4	15.4	6.8	11.1	15.5	6.8	11.1	15.6	6.8	11.2
144.8	15.1	6.7	9.2	15.3	6.7	11.1	15.4	6.8	11.1	15.5	6.8	11.1
152.3	15.0	6.7	9.1	15.2	6.7	11.1	15.3	6.7	11.1	15.4	6.8	11.1
161.3	14.9	6.7	9.0	15.0	6.7	11.0	15.2	6.7	11.1	15.3	6.7	11.1

Unlike PMMA and PC, little data are available in the literature regarding the sorption of CO_2 by PVB. At the time of this work, only one sorption study had been identified in the literature, conducted at $T = 25^oC$ and pressures up to 40 bar,[513] well below the critical point of CO_2 (31.1^oC and 73.8 bar). These data, reproduced in Table 6-23.

Table 6-23. *Literature values of CO_2 sorption in PVB.*

T (^{o}C)	P (bar)	[CO_2] $\left(cm^3 STP \middle/ cm^3\ polymer \right)$	Ref
25	0	0.00	512
25	5.8	8.70	"
25	10.9	15.20	"
25	20.3	26.90	"
25	*30.4*	*38.70*	"
25	35.5	45.70	"

This lack of CO_2 sorption, from which PVB swelling would be determined, does not allow for a calculation of PVB HSP values due to CO_2 sorption. However, it can be observed from the HSP values calculated for PVB as a function of T and P, Table 6-22, little change is noted in the polar or hydrogen bonding values. And while it was observed with PMMA and PC that swelling of these polymers with CO_2 lowers the HSP dispersion value significantly, lesser effects where observed for the polar and hydrogen bonding parameters. This tendency, makes it unlikely that swelling of PVB at the temperatures and pressures of the experiments (to be reviewed in Chapter 8) will lower the polar and hydrogen bonding PVB HSP values to a range comparable with pure CO_2 or, indeed, a CO_2-rich solvent. Also, of the three polymers involved in the current applications, PVB is likely to behave as a Lewis acid in the presence of CO_2 (also a Lewis acid), as a result of the large amount of hydroxyl in the polymer, Figure 6-13. Further, as can be seen from the HSP values, the high value of the hydrogen bonding component indicates some degree of intra-molecular hydrogen bonding (or self association), possibly between the hydrogen of the hydroxyl groups and the carbonyl oxygen in the acetyl groups.

The ambient conditions T_g of PVB varies from 51 to 90°C depending on the hydroxyl content and as can be seen in Figure 6-15, the T_g of PVB can be depressed as a result of CO_2 sorption, which can be expressed by

$$T_g(^\circ C) = -0.7975 \cdot \left[CO_2 \left(cm^3 \; STP \Big/ cm^3 \; polymer \right) \right] + 51 \qquad (6\text{-}21)$$
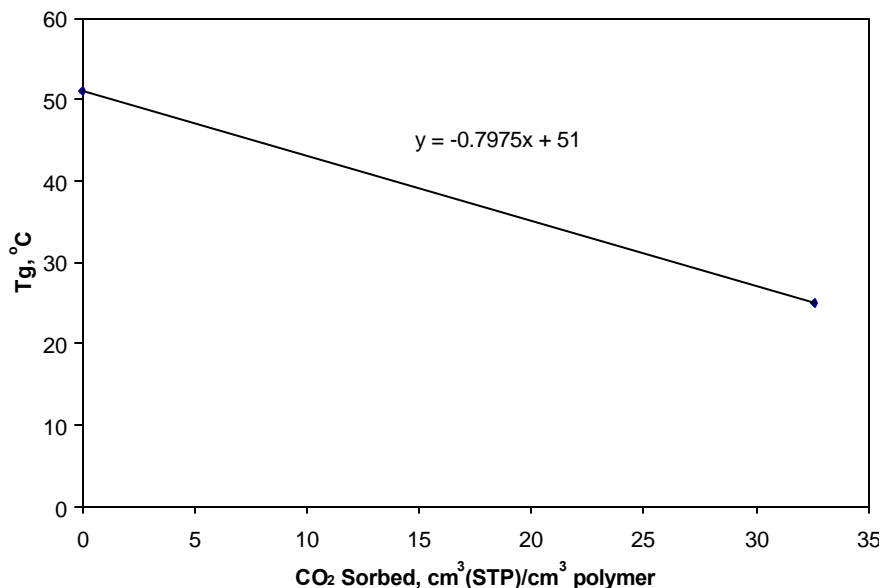
Figure 6-15. T_g depression in PVB due to CO_2 sorption.

From the 25°C CO_2 sorption data listed in Table 6-23, the PVB begins its transition from a glass state to a rubber state with the sorption of 32.6 cm³(STP)/cm³ polymer. As indicated by the bold, italic type, the PVB is assumed to be plasticized in a CO_2 environment at 25°C and 30.4 bar.

The partial molar volumes of CO_2 dissolved in PVB are calculated using eqn. 6-8, and are given in Table 6-24.

Table 6-24. Calculated partial molar volumes of CO_2 dissolved in PVB.

T (°C)	P (bar)	Internal Pressure, PC (bar)	$\overline{V}_{CO_2} \left(cm^3 / mol \right)$
50	100	4473.2	37.9
50	200	4528.4	37.5
100	100	4214.8	40.1
100	200	4260.1	39.6
Average			38.8

In comparing PVB to PMMA and PC, it can also be seen from Table 6-24, that the internal pressure of PVB for comparable temperatures and pressures are higher than PMMA or PC. This result is also depicted in the higher HSP values of PVB in comparison to PMMA and PC.
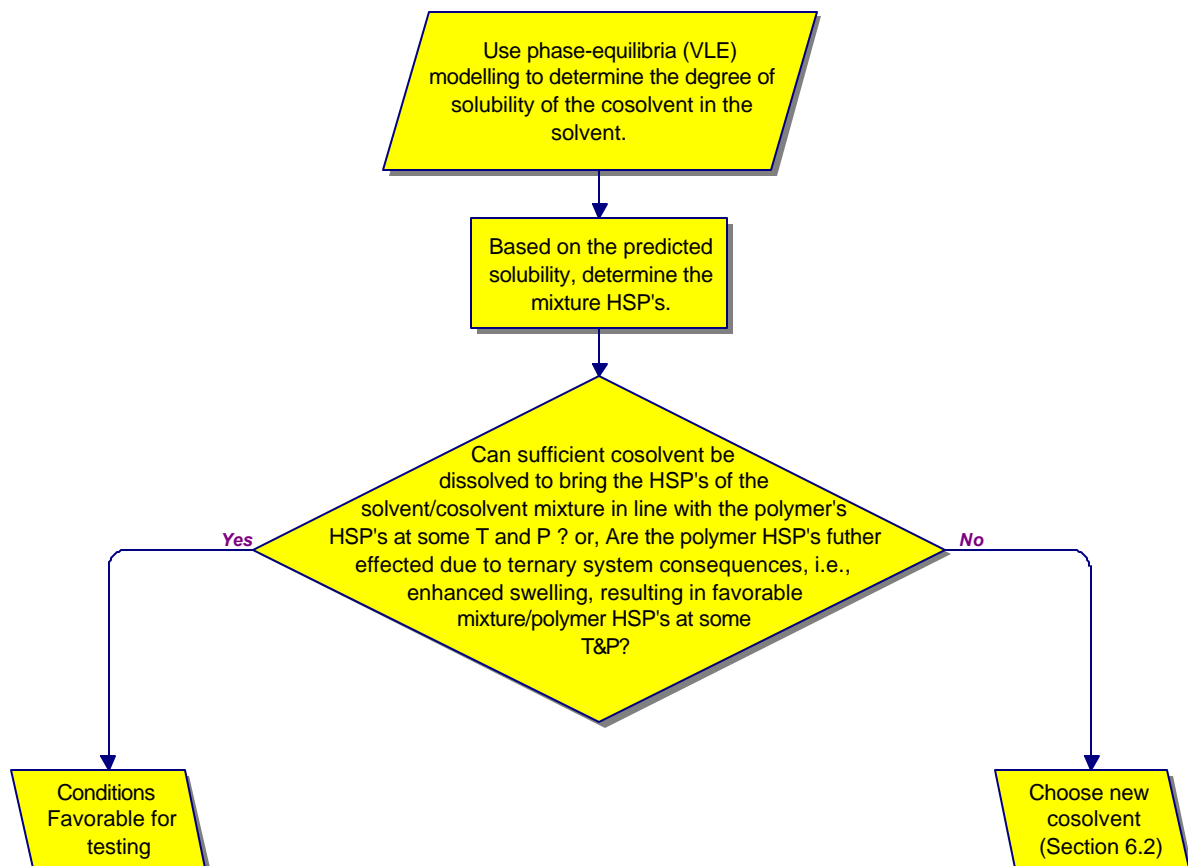
6.2 Cosolvent/Polymer Interactions
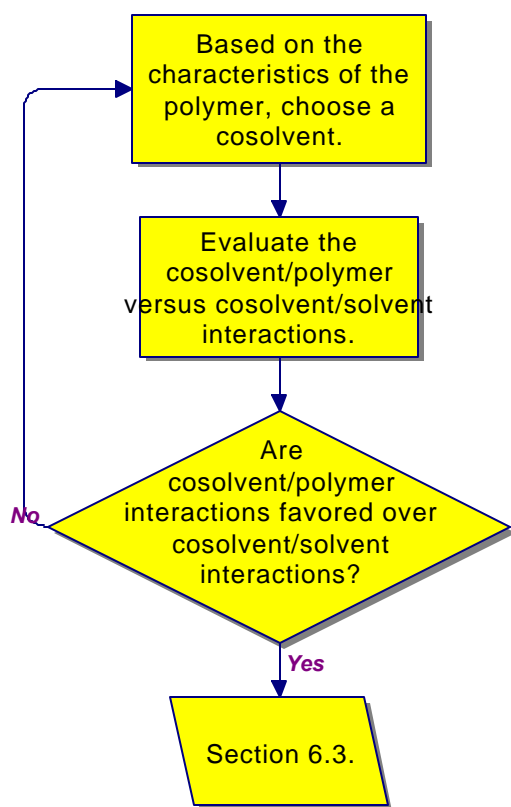
Figure 6-16. Cosolvent/polymer decision tree.

The addition of a small amount of cosolvent, in addition to altering the chemical nature of the solvent (CO_2), has also been reported to enhance the swelling of polymers subjected to modified supercritical CO_2.[514,515,516] In research recently published by West

et al.,[517] poly(dimethyl siloxane) was swollen by a CO_2/acetone mixture by almost 600%. At the same conditions of temperature and pressure, this is a nearly 5-fold increase over the swelling caused by pure CO_2. The authors of this work attribute the enhanced swelling effect to strong interactions of the cosolvent with the polymer. Further, the less volatile cosolvent may partition preferentially into the polymer phase, especially if favorable interactions between the polymer and cosolvent, such as hydrogen bonding or Lewis acid/base formations exist, and may block active sites, thus precluding polymer/polymer interactions.[518] Work in quantifying and studying the partitioning of cosolvents between supercritical CO_2 and polymer phases is currently ongoing using in situ Fourier transform IR and UV-vis spectroscopy. This methodology has allowed not only the quantification of partitioning, but also the ability to identify the type of interactions playing a role in the partitioning. The increased sorption of methanol in PMDS was attributed to hydrogen bonding between the methanol hydroxyl functional groups and the basic sites of PMDS with this technique.[519] Others researchers using mass spectrometry tracer pulse chromatography reported a C_{18} bonded phase in contact with 2 mol% methanol modified CO_2 was composed of up to 25 mol% methanol near the critical mixture region, and that at all conditions of temperature and pressure the concentration of methanol in the C_{18} bonded phase always exceeded the concentration in the supercritical fluid phase.[520]

6.3 Solvent/Cosolvent Interactions

Figure 6-17. *Solvent/cosolvent decision tree.*

As previously mentioned, to enhance CO_2 solubility and disrupt polymer/polymer interactions, a second compound or modifier, may be added to supercritical CO_2 as a cosolvent. The addition of a small amount of cosolvent can also significantly enhance solute solubility if specific interactions exist between the cosolvent and solute. Electrostatic interactions between the cosolvent and solute may include all of the *van der Waals* interactions mentioned previously. When using a polar cosolvent for polar solutes, specific chemical interactions like hydrogen bonding or charge transfer complex

formation can also lead to large cosolvent effects.[521] However, it must be remembered when selecting a cosolvent that the solvent can compete with the solute for the cosolvent. This is because CO_2 has two carbonyl oxygens that will accept hydrogen bonds and generally the supercritical solvent is in excess in the solution so that if the solvent can compete for specific interaction sites, as the CO_2 can, it will hydrogen bond to the cosolvent before the cosolvent can affect solute solubility levels.[522] Such interactions tie up hydrogen-bonding sites that might otherwise be available for interactions between the polymer and cosolvent. This competition between solvent/cosolvent and cosolvent/solute interactions must therefore be considered when choosing a cosolvent, particularly when the solvent has donor-acceptor properties.

Solubility parameter values for a number of compounds, which could be used as cosolvents, are tabulated in various references, or can be determined using the methods outlined in Section 5.4. Once the solubility parameters for the solvent (CO_2) and cosolvent have been assigned, a solubility parameter for the solvent-cosolvent mixture can be calculated using a volume average

$$d_m = \frac{f_1}{f_1 + f_2} d_1 + \frac{f_2}{f_1 + f_2} d_2 \qquad (6\text{-}22)$$

where d_1 and d_2 refer to the solvent and cosolvent solubility parameters respectively, and f_1, f_2 refer to the respective volume or mole fractions.[523,524,525,526,527,528]

Determination of the volume fraction of solvent and cosolvent is accomplished through a calculation of the vapor-liquid equilibrium for the solvent (CO_2) - cosolvent system of interest. In this work, a cubic EOS, with temperature-independent mixing rules

is used. Chapter 7 illustrates the use of this EOS to model the VLE for the CO_2-propylene carbonate system, where new phase equilibria data are presented. These new data extends the range of pressures into the supercritical fluid region of CO_2.